People's Democratic Republic of Algeria
Ministry of Higher Education and Scientific Research
Echahid Cheikh Larbi Tebessi University – Tebessa-
Faculty of Exact Sciences and Natural and Life Sciences
Department of Applied Biology

Field: Natural and Life Sciences

Thesis

Presented with a view to obtaining the Master's degree
In: Toxicology

Entitled:

Impairment of renal mitochondria by nanoparticles

By:

Haoues Ouijdene ***Zoghlami Nour El Houda***

Jury:

Mr. Gasmi S.	Ecahahid Cheikh Larbi Tebessi	President
Mr. Rouabhi R.	Ecahahid Cheikh Larbi Tebessi	Reporter
Dr. Taib Ch.	Ecahahid Cheikh Larbi Tebessi	Examiner

Graduation day: 11-06-2025.


بسم الله الرحمن الرحيم

Acknowledgement

First and foremost, we thank **Allah**, the Most Merciful, for granting us the strength, patience and clarity throughout this journey. Without His guidance we
wouldn’t achieve this.

We express our sincere and profound gratitude to **Professor Rouabhi Rachid**, whose trust, wisdom, and patient mentorship were essential to the success of this research. May he see in this humble work a sincere tribute to the greatness of his
character and the precision of his scientific vision.

Our sincere thanks also go to **Mr. GASMI Salim**, President of the jury, and **Mrs. TAIB Chahinez**, our examiner. Having been our teachers in earlier years, their continued presence in our academic journey is both a source of pride and a continuation of their invaluable teaching legacy. We are truly grateful for their efforts and lasting impact on our formation.

Finally, we warmly thank all those who contributed to the realization of this study, whether through advice, encouragement, or technical assistance, each gesture helped bring this endeavor to completion

Dedication

To the ones who were there, and the ones who weren’t.

To interruptions, delays, and things that didn’t go as planned.

We moved through it,

Sometimes crawling, sometimes guessing.

Somehow, this exists now.

Abstract

This study investigates the toxicological impact of nickel dioxide nanoparticles (NiO_2 NPs) on renal mitochondrial function and oxidative stress biomarkers in Wistar rats. Animals were administered NiO_2 NPs orally at two doses (5 and 15 mg/kg/day) over a defined treatment period (20 days).

Biochemical evaluations revealed dose-dependent disruptions**.** Total protein levels increased at 5 mg but decreased at 15 mg, while lipid levels consistently declined at both doses, suggesting membrane damage. Malondialdehyde (MDA) levels increased significantly, while reduced glutathione (GSH) levels decreased at both doses, reflecting elevated oxidative stress.

Antioxidant enzyme activities (GST, GPx, CAT) were upregulated at 5 mg but markedly suppressed at 15 mg, indicating enzymatic exhaustion at higher exposure. Mitochondrial assessments revealed increased swelling at both doses and a dose-dependent decline in mitochondrial respiration, highlighting mitochondrial dysfunction.

In conclusion, NiO_2 nanoparticles induce oxidative stress, impair mitochondrial bioenergetics, and trigger nephrotoxic effects in a dose-dependent manner in Wistar rats.

Keywords : Nickel dioxide nanoparticles, oxidative stress, renal mitochondria, antioxidant enzymes, mitochondrial dysfunction, Wistar rats, nephrotoxicity.

Résumé

Cette étude explore les effets toxiques des nanoparticules de dioxyde de nickel (NPs NiO_2) sur la fonction mitochondriale rénale et les biomarqueurs du stress oxydatif chez le rat Wistar. Les animaux ont reçu des doses orales de 5 et 15 mg/kg/jour pendant une période expérimentale définie (20 jours).

Les analyses biochimiques ont révélé des altérations dose-dépendantes. Le taux de protéines totales a augmenté à 5 mg puis diminué à 15 mg, tandis que les lipides ont diminué aux deux doses, traduisant une altération membranaire. Le MDA a augmenté de manière significative, et le GSH a diminué, indiquant un stress oxydatif accru.

Les activités des enzymes antioxydantes (GST, GPx, CAT) ont augmenté à 5 mg mais ont été fortement inhibées à 15 mg, ce qui suggère une saturation du système antioxydant enzymatique. L'analyse mitochondriale a montré une augmentation du gonflement mitochondrial aux deux doses et une réduction de la respiration mitochondriale proportionnelle à la dose, indiquant un dysfonctionnement mitochondrial.

En conclusion, les nanoparticules de NiO_2 induisent un stress oxydatif, perturbent la fonction bioénergétique des mitochondries rénales et provoquent une toxicité rénale dépendante de la dose chez le rat Wistar.

Mots clés : Nanoparticules, dioxyde de nickel, stress oxydatif, mitochondries rénales, enzymes antioxydantes, dysfonctionnement mitochondrial, rats Wistar, toxicité rénale.

الملخص

تهدف هذه الدراسة إلى تحليل التأثيرات السمية لجسيمات ثاني أكسيد النيكل النانوية (NiO_2 NPs) على وظيفة الميتوكوندريا الكلوية ومؤشرات الإجهاد التأكسدي لدى فئران ويستار .تم إعطاء الجرعات عن طريق الفم بتركيزين (5 و15 ملغ/كغ/يوم) خلال فترة علاج محددة (20 يوم).

أظهرت التحاليل الحيوية تغيرات تعتمد على الجرعة . زادت مستويات البروتين الكلي عند جرعة 5 ملغ ثم انخفضت عند

15 ملغ، في حين انخفضت مستويات الدهون في كلا الجرعتين، مما يشير إلى تلف الأغشية. ارتفع مستوى المالونداياالديهيد (MDA) بشكل ملحوظ، بينما انخفض الجلوتاثيون المختزل (GSH) ، مما يدل على إجهاد تأكسدي واضح.

الأنزيمات المضادة للأكسدة (GST، GPx، CAT) أظهرت نشاطًا مرتفعًا عند جرعة 5 ملغ، ثم انخفضت بشكل حاد عند 15 ملغ، مما يشير إلى إنهاك الدفاع الأنزيمي. كما كشفت النتائج عن زيادة في انتفاخ الميتوكوندريا في كلتا الجرعتين، مع انخفاض في معدل التنفس الميتوكوندري يتناسب مع الجرعة، ما يدل على خلل في وظيفة الميتوكوندريا.

تشير النتائج إلى أن جسيمات NiO_2 النانوية تسبب إجهادًا تأكسديًا، وتضعف وظائف الميتوكوندريا الكلوية، وتؤدي إلى سمية كلوية تعتمد على الجرعة لدى فئران ويستار.

الكلمات المفتاحية: جسيمات نانوية، ثاني أكسيد النيكل، الميتوكوندريا الكلوية، الإجهاد التأكسدي، إنزيمات مضادة للأكسدة، خلل في وظيفة الميتوكوندريا ، فئران ويستار، السمية الكلوية.

Abbreviations list

% : Percent

< : Less than

≤ : Less than or equal to

= : Equals

> : Greater than

~ : Approximately

°C : Degrees Celsius

Δψm : Mitochondrial Membrane Potential 8-OHdG : 8-Hydroxy-2'-deoxyguanosine

AD : *Anno Domini* (years after Christ's birth) ADP : Adenosine Diphosphate

AINPs : Aluminum Oxide Nanoparticles AKI : Acute Kidney Injury

ATP : Adenosine Triphosphate Bcl-2 : B-cell lymphoma 2

Cm : Centimeter

CuNPs : Copper Nanoparticles Cu_2O : Copper(I) Oxide

DNA : Deoxyribonucleic Acid

DLVO : Derjaguin Landau Verwey Overbeek
DMT : Derjaguin Muller Toporov

DTNB : 5,5′-Dithiobis(2-nitrobenzoic acid)

DW1/AD : Electrode chamber (for oxygen measurement)

e.g. : *Exempli gratia* (for example) EDTA : Ethylenediaminetetraacetic Acid EM : Electron Microscopy

$FADH_2$: Flavin Adenine Dinucleotide GFB : Glomerular Filtration Barrier

g : Gram

GI : Gastrointestinal HCl : Hydrochloric Acid IL-18 : Interleukin-18 J/g : Joules per gram

$J\ g^{-1}\ K^{-1}$: Specific heat capacity

JC-1 : Mitochondrial membrane potential-sensitive dye Kg : Kilogram

KIM-1 : Kidney Injury Molecule-1 L : Liter

mL : Milliliter mg : Milligram min : Minute mM : Millimolar

mtDNA : Mitochondrial DNA µg : Microgram

µL : Microliter
µM : Micromolar µmol : Micromole µm : Micrometer

NaCl : Sodium Chloride NaOH : Sodium Hydroxide N : Normality

NADH : Nicotinamide Adenine Dinucleotide (reduced form) NGAL : Neutrophil

Gelatinase-Associated Lipocalin

Ni^{2+} : Nickel ion

NiNP : Nickel Nanoparticles NiO_2 : Nickel Dioxide

nm : Nanometer NPs : Nanoparticles

OCR : Oxygen Consumption Rate P : Probability value

PBS : Phosphate-Buffered Saline PbS : Lead(II) Sulfide

PINK1 : PTEN-Induced Kinase 1 PVP : Polyvinylpyrrolidone

QDs : Quantum Dots

rpm : Revolutions per minute ROS : Reactive Oxygen Species TBS : Tris-Buffered Saline

TCA-BHT : Trichloroacetic Acid–Butylated Hydroxytoluene V : Volume

WHO : World Health Organization

$W\ m^{-1}\ K^{-1}$: Thermal conductivity (Watts per meter per Kelvin) ZnO : Zinc Oxide

List of Figures

Figure 1: The Lycurgus Cup under reflected light (A, green) and transmitted light (B, red-purple).....4
Figure 2: Structural illustrations of various nanoparticles used in biomedical research....5
Figure 3: different types of nanoparticles **(Haleem et *al*., 2023).**.....7
Figure 4: Biodistribution of nanoparticles in the body **(Viala & Botta, 2005)**. 10
Figure 5: Raw Nickel Sample **(MAT, 2023)** 13
Figure 6: Structural Organization of a Mitochondrion **(Bassaglia, 2004).** 16
Figure 7: Mitochondrial Dynamics and Targets for Oxidative Damage **(Ho & Shirakawa, 2023).**.....19
Figure 8: Animal material **(personal picture)**.....24
Figure 9: Rat Food "Croquettes" **(personal picture)** 25
Figure 10: Rat distribution **(personal picture).**.....25
Figure 11: Weight measurement **(personal picture).**.....27
Figure 12: sacrifices of rats **(personal picture).**.....27
Figure 13: sacrifice and kidney removal **(personal picture).**.....28
Figure 14: Summary Diagram of the Experimental Protocol.....30
Figure 15: Extraction methods and assay of major biochemical constituents (lipids, proteins.) .32
Figure 16: Evolution of the body weight in rats treated for 20 days with NiO_2 NPs.....40
Figure 17: Evolution of the relative weight of the brain in rats treated for 20 days with NiO_2 NP. 41
Figure 18: Variation in kidney protein levels of control and treated rats after 20 days of NiO_2 NP exposure.....42
Figure 19: Variation in kidney lipid levels of control and treated rats after 20 days of NiO_2 NP exposure.....42
Figure 20: Variation in MDA levels in the kidneys of control and treated rats after 20 days of treatment. 43
Figure 21: Variation in GSH levels in the kidneys of control and treated rats after 20 days of treatment. 44
Figure 22: Variation in kidney GST activity in control and NiO_2 NP-treated rats after 20 days of exposure. 44
Figure 23: Variation in catalase (CAT) activity in the kidneys of control and NiO_2 NP-treated rats after 20 days of exposure.....45
Figure 24: Variation in glutathione peroxidase (GPx) activity in the kidneys of control and NiO_2

NP-treated rats after 20 days of exposure. 46
Figure 25: Variation in renal mitochondrial swelling of control and NiO_2 nanoparticle-treated rats after 20 days of treatment. 47
Figure 26: variation in renal mitochondrial respiration of control and NiO_2 nanoparticle treated rats after 20 days of treatment. 47

Liste of tables:

Table …….. page
Table 01: Physical Properties of nickel**……**13.

Table of contents

Acknowledgement.....-

Dedication.....-

Abstract.....-

Résumé.....-

الملخص.....-

List of Figures.....-

Introduction.....1

Part I: Generalities and definitions

Chapter 01: General overview of Nanoparticles.....

1. Historical Overview of Nanoparticles.....4
2. Definion of Nanoparticles.....5

3.Classifications of Nanoparticles.....6

3.1. Organic NPs.....6

3.2. Inorganic NPs.....6

3.3. Carbon-based NPs.....6

4. Uses of nanoparticles.....7
5. Physicochemical properties of nanoparticles.....7

5.1. Mechanical properties.....7

5.2. Thermal properties.....8

5.3. Electronic and optical properties.....8

6 .Toxicokinetic of nanoparticles.....8

6.2.Distribution.....9

6.3. Metabolism.....9

6.4. Excretion.....9

7. Nanotoxicity.....10
8. Impact of NPs on Biological Systems.....11

Chapter 02: Toxicological impact of Nanoparticles on renal mitochondria.....,

1. Definitions and fundamental concepts.....12

1.1. Nickel (Ni).....12

1.1.2. Nickel in Soil: Occurrence and Bioavailability.....12

1.1.3. Sources, Uptake, and Health Risks of Nickel.....12

1.1.4. Physical Properties.....13

1.2. Nickel Dioxide (NiO_2).....13

1.3. Nephrotoxicity of Nanoparticles 14
1.3.2. Biomarkers of Nephrotoxicity 14
1.3.3. The implication of nephrotoxicity 15
1.3.3.2. Accumulation in renal tissues and filtration pathways 15
1.4. Bioenergetics 15
1.5. Mitochondrial Dysfunction: Its Role in Renal Pathophysiology 15
1.5.2. Role of Mitochondria: 16
1.5.4. Role of Renal Mitochondria in Kidney Function 17
1.6. Oxidative stress 17
1.6.2. Oxidative Stress and Mitochondrial Impairment in Renal Pathologies 18
2. Mechanisms of Nanoparticle-Induced Mitochondrial Toxicity 19
2.2. Effects on Mitochondrial Membrane Potential (Δψm) 19
2.3. Induction of Mitochondrial Permeability Transition Pore (mPTP) 19
2.4. Damage to Mitochondrial DNA (mtDNA) 20
2.5. Impairment of Mitochondrial Dynamics 20
3. Autophagy and Mitophagy in Response to Nanoparticle Exposure 20
3.2. Mitochondrial Quality Control via Mitophagy 20
3.3. Dysregulation of Mitophagy in Kidney Cells 21
4. Techniques for Assessing Mitochondrial Impairment 21
4.2. Electron Microscopy and Mitochondrial Imaging 21
4.3. Assays for Mitochondrial Function 22

Part II: Materials, methods & experimental study

1.1.2. Chemical material 24
1.1.3. Animal Diet 24
1.2. Methodology 25
1.2.2. Justification for Dose Selection 26
1.2.3. Preparation of the solution 26
1.2.4. Weight measurement 26
1.2.5. Treatment of rats 27
1.2.6. Sacrifice and taking of samples 27
1.3. Methods of dosage 31
1.3.1. Determination of biochemical parameters 33
1.3.2. Oxidative stress parameters 34
1.3.2.1. Non-enzymatic biomarkers 34

1.3.2.2. Enzyme biomarkers: 36
1.4. Statistical Analysis 39

RESULTS .....

1. Results 40
1.1.1. Weight gain 40
1.1.2. Relative kidney weight 40
1.2. Effect of Nickel dioxide treatment on kidney metabolites 41
1.2.1. Effect on kidney protein levels 41
1.2.2. Effect on the lipid level of the kidney 42
1.3. Treatment effect on non-enzymatic parameters 42
1.3.2. Effect of treatment on the level of GSH 43
1.4. Effect of NiO_2 nanoparticle exposure on enzymatic parameters in the kidneys of rats 44
1.4.3. Effect of NiO_2 nanoparticle treatment on glutathione peroxidase activity in the kidneys of rats 45
1.5. Effect on mitochondria 46
1.5.2. Mitochondrial Respiration 47

DISCUSSION .....

1. Discussion 48
1.1. Effect on body weight 48
1.2. Effect on Kidney Weight 49
1.3. Effects on the rate of metabolites 49
1.3.2. Effects on lipid levels 50
3.3. Effects on the rate of biomarkers of oxidative stress 51
3.3.2. Effect of Nio2 nanoparticle on glutathione peroxidase (GPX) 51
3.3.3. Effect of Nio2 nanoparticle on catalase. 52
3.3.4. Effect on the level of Malondialdehydes, ... 52
3.3.5. Effect of NiO_2 nanoparticle exposure on GST 53
1.4. Effect on Mitochondrial swelling 54

CONCLUSION **58**

REFERENCES **60**

Introduction

Introduction

The growing field of nanotechnology has led to the extensive use of nanoparticles (NPs) across various sectors, including medicine, electronics, and environmental sciences. Nickel nanoparticles (Ni-NPs), in particular, are widely utilized due to their distinct physicochemical properties, making them essential in applications like catalysts, sensors, and batteries. However, their increasing use raises significant concerns regarding their potential toxicity, especially their harmful effects on kidney function and mitochondrial integrity. Investigating the toxicological impact of Ni-NPs is crucial to understanding their interactions with biological systems and assessing the risks they pose to human health **(Zhang et *al*., 2022)**.

Although the production and use of nickel oxide nanoparticles (NiONPs) are widespread, environmental and public health problems are associated with them. The kidney is the primary organ responsible for excretion and is one of the main targets of nanoparticle-induced toxicity **(Karaboduk et *al*., 2024)**. The kidneys are a pair of bean-shaped organs responsible for regulating blood volume, eliminating waste, maintaining overall fluid balance, and filtering minerals from the bloodstream. Positioned on either side of the spine in the retroperitoneal space, the kidneys typically measure 6 cm in width, 11–14 cm in length, and 4 cm in thickness. Each kidney contains approximately 1.3 million nephrons, which serve as its functional units **(Waris et *al*., 2023).**

Nickel nanoparticles (Ni-NPs) have been identified as nephrotoxic agents, primarily due to their capacity to induce oxidative stress and activate apoptotic pathways. Exposure to Ni-NPs leads to an elevated production of reactive oxygen species (ROS), resulting in lipid peroxidation, and the initiation of apoptosis. Research indicates that ROS generation is a central mechanism by which Ni-NPs exert nephrotoxic effects, causing oxidative stress and subsequent cellular apoptosis **(Siddiqui et *al*., 2012)**. Ni-NPs have also been reported to alter enzyme activity and modulate gene expression, which plays a significant role in their overall toxicity **(Du et *al*., 2024)**. A clear understanding of these mechanisms is crucial for formulating preventive strategies and regulatory policies to reduce the adverse health impacts of Ni-NP exposure **(Zhang et *al*., 2022).**

Mitochondria, as the primary energy-generating organelles within cells, play a crucial role in maintaining cellular function and survival. Disruption of mitochondrial integrity can have severe toxicological consequences, particularly in metabolically active organs such as the kidneys.

Exposure to Ni-NPs has been directly linked to mitochondrial dysfunction in renal cells, both in vitro and in vivo. Studies have shown that Ni-NPs induce oxidative stress, inflammation, calcium imbalances, and mitochondrial damage, ultimately leading to cellular injury and impaired kidney function **(Abd-Eltawab Tammam et *al*., 2022).**

The integration of nanotechnology into various sectors necessitates a thorough assessment of the toxicological implications associated with nanoparticle exposure, particularly concerning renal health **(Zhang et *al*., 2022)**. Given the potential hazards linked to Ni-NP exposure, ongoing research is crucial to determine safe exposure thresholds and implement effective risk mitigation strategies. Investigating the dose-dependent toxicity of Ni-NPs and their prolonged impact on kidney function will contribute to the progress of nanotoxicology and the development of regulatory frameworks. By fostering collaboration between nanotechnology and biomedical research, it becomes possible to maximize the advantages of nanoparticles while reducing their harmful effects, ultimately promoting safer applications across medicine, industry, and environmental sciences **(Waris et *al*., 2023)**.

In this research, we have focused our efforts on studying the toxicity of nickel dioxide nanoparticles (NiO_2 NPs) and their potential to impair mitochondrial function in the kidneys, using Wistar rats as our experimental model. Our approach aimed to simulate exposure conditions and evaluate how these nanoparticles affect renal bioenergetics and oxidative balance. Specifically, our work involved:

- Exploring the toxicological effects of NiO_2 NPs on renal mitochondria.
- Assessing oxidative stress parameters such as MDA, GSH, CAT, GST, and GPx.
- Measuring biochemical and metabolic changes in the kidney including protein and lipid levels.
- Monitoring physiological changes like body weight and relative kidney weight.
- Evaluating mitochondrial-specific responses such as swelling and respiratory function.

This thesis is divided into two main sections. The first part provides the general framework and theoretical background. It begins with an overview of nanoparticles, their definitions, types, uses, and physicochemical properties, before moving on to discuss their toxicokinetics and biological interactions. A special focus is placed on nickel and nickel dioxide nanoparticles, their

nephrotoxicity, and the role of mitochondria in renal physiology. We also examine key concepts such as oxidative stress, mitochondrial dysfunction, and nanoparticle-induced toxicity mechanisms.

The second part is dedicated to the experimental study. It outlines the materials and methods used in our investigation, including the justification of the chosen doses, treatment protocols, and techniques for measuring biochemical and oxidative stress parameters. Finally, we present our results, followed by a detailed discussion that connects our findings with existing literature. The thesis concludes by summarizing the outcomes and emphasizing the broader significance of understanding nanoparticle-induced renal mitochondrial toxicity.

Part I:
Generalities and definitions

Chapter 01:
General overview of Nanoparticles

1. Historical Overview of Nanoparticles

The use of nanostructured materials can be traced back to the 4th century AD, notably by the Romans, who unintentionally applied nanoscale technology in their craftsmanship. A prime example is the Lycurgus Cup, part of the British Museum's collection, which stands as a remarkable testament to ancient glass-making expertise. This artifact is the earliest known instance of dichroic glass; a material that displays different colors depending on the lighting conditions. Specifically, the cup appears green when illuminated with reflected light, and reddish-purple when light passes through it, a phenomenon resulting from the presence of gold and silver nanoparticles embedded in the glass matrix. In 1990, researchers employed transmission electron microscopy (TEM) to reveal that the Lycurgus Cup's color changing effect is caused by Ag-Au alloy nanoparticles (50– 100 nm) embedded in the glass. The red-purple color results from gold nanoparticle absorption, while the green comes from silver nanoparticle scattering. This cup is one of the earliest synthetic nanomaterials, and a similar effect appears in medieval stained glass due to embedded metal nanoparticles **(Bayda et *al*., 2020)**.



Figure 1: The Lycurgus Cup under reflected light (A, green) and transmitted light (B, red-purple)

Humans have used nanomaterials for millennia. Over 4,500 years ago, asbestos nanofibers were added to ceramic matrices, and ancient Egyptians synthesized lead sulfide (PbS) nanoparticles (~5 nm) for use in hair dye. They also developed the pigment Egyptian blue, composed of nanoscale glass and quartz, which was widely used for decoration. By the 14th century BC, metallic

nanoparticles were deliberately created during glass production. Examples include red glass colored by copper nanoparticles and Celtic red enamels containing cuprite (Cu_2O). Mesopotamians also used metallic nanoparticles for luster decoration in glazed ceramics, creating iridescent effects with layered silver and copper nanoparticles. In the 19th century, similar methods were used in Japan to produce ruby-colored Satsuma glass using copper nanoparticles. Even natural nanomaterials such as clay were employed as early as 5000 BC to bleach textiles in Cyprus **(Jeevanandam et *al*., 2018)**.

2. Definion of Nanoparticles

The word "nanoparticle" combines "nano-" from the Greek nanos (νᾶνος), meaning "dwarf" or "tiny," and "particle," referring to a small unit of matter. This term highlights the extremely small size of nanoparticles, which measure between 1 and 100 nanometers in at least one dimension **(Buzea et *al*., 2007)**.

Nanoparticles can originate naturally or be synthesized through human activities. Their diminutive scale imparts unique physical and chemical properties, such as enhanced reactivity and distinct optical characteristics, which differ markedly from their bulk counterparts. These attributes render them highly valuable across various sectors, including medicine, engineering, catalysis, and environmental remediation **(Khan et *al*., 2019).**

The synthesis of nanoparticles encompasses a diverse array of materials, such as metals, semiconductors, ceramics, and polymers. By meticulously adjusting parameters like size, shape, and surface characteristics during fabrication, scientists can tailor nanoparticles to meet specific application requirements. This customization is pivotal in optimizing their performance for targeted uses **(Salata, 2004).**

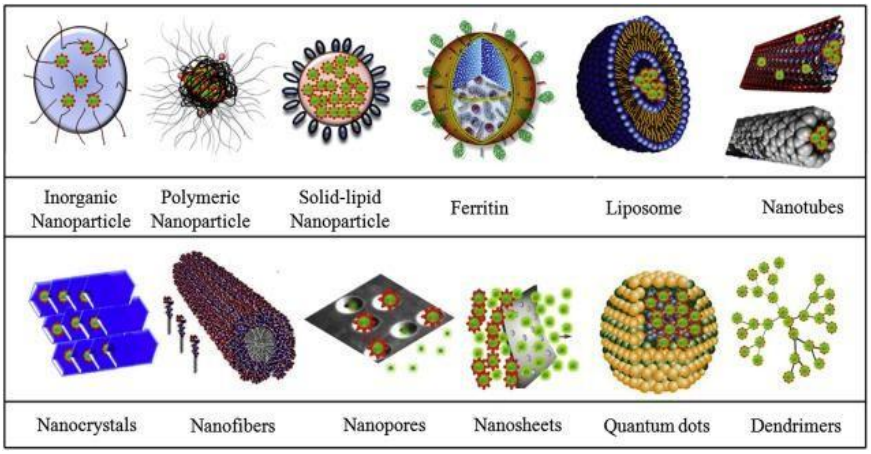


Figure 2: Structural illustrations of various nanoparticles used in biomedical research **(Muthuraman & Kaur, 2017).**

3. Classifications of Nanoparticles

Nanoparticles (NPs) are typically classified into three categories based on their composition: organic, carbon-based, and inorganic.

3.1. Organic NPs

Organic nanoparticles (NPs) are composed of proteins, carbohydrates, lipids, or polymers, with common examples including dendrimers, liposomes, micelles, and protein complexes. They are generally biodegradable, non-toxic, and, in some cases, possess a hollow core. These NPs are sensitive to heat and light and are often formed through non-covalent interactions, making them more labile and easier to clear from the body. Their applications depend on factors like composition, surface morphology, stability, and carrying capacity. Currently, they are widely used in biomedical fields, particularly for targeted drug delivery and cancer therapy **(Joudeh & Linke, 2022).**

3.2. Inorganic NPs

Inorganic nanoparticles (NPs) consist of non-carbon-based materials such as metals, ceramics, and semiconductors. Metal NPs can be monometallic, bimetallic, or polymetallic, possessing unique optical, electrical, thermal, and magnetic properties due to localized surface plasmon resonance, making them essential for biomedical, pharmaceutical, and technological applications. Semiconductor NPs have tunable bandgaps, making them suitable for photocatalysis, optics, and electronic devices. Ceramic NPs, composed of oxides, carbides, phosphates, and carbonates, are highly stable with a high load capacity, making them valuable in biomedical applications, catalysis, dye degradation, and optoelectronics **(Joudeh & Linke, 2022).**

3.3. Carbon-based NPs

Carbon-based nanoparticles (NPs), including fullerenes, carbon black, and carbon quantum dots, exhibit unique electrical, optical, and thermal properties. Their high conductivity, strength, and biocompatibility make them valuable in drug delivery, bioimaging, energy storage, and environmental sensing. More complex forms, like nanodiamonds and carbon nano-onions, are particularly useful in tissue engineering and medical applications due to their low toxicity **(Joudeh & Linke, 2022).**

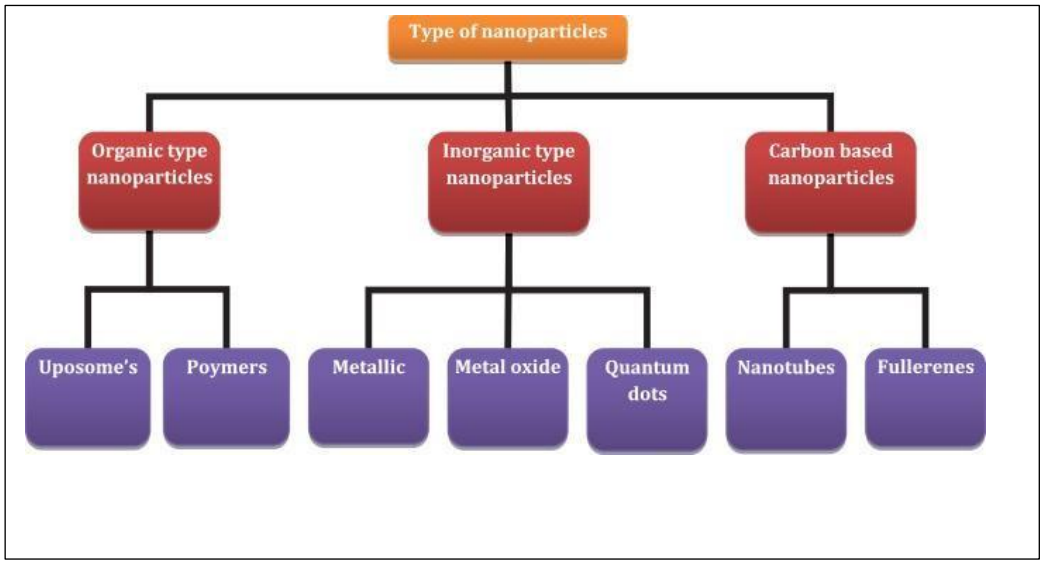


Figure 3: different types of nanoparticles **(Haleem et *al*., 2023).**

4. Uses of nanoparticles

Nanoparticles have various biomedical applications, including fluorescent labeling for detecting biological markers in disease research and diagnosis. They are essential in drug and gene delivery systems, aiding targeted therapies. Additionally, they are used for detecting pathogens, analyzing proteins, and isolating biological molecules and cells. Nanoparticles also contribute to DNA probing, genetic and tissue engineering, and tumor treatment through drug or heat-based therapies. Moreover, they enhance imaging techniques like MRI and support pharmacokinetic studies for drug development **(Salata, 2004)**.

5. Physicochemical properties of nanoparticles

Nanoparticles (NPs) are widely used due to their unique physical and chemical properties, which differ from those of their larger counterparts. The upcoming text highlights the key physicochemical properties that undergo changes at the nanoscale:

5.1. Mechanical properties

Mechanical properties define how a material behaves under various external forces and conditions. In nanomaterials, these properties differ significantly from bulk materials due to surface and quantum effects. Traditional materials exhibit characteristics such as strength, hardness, brittleness, flexibility, and rigidity, with inorganic materials often being brittle and

organic materials generally more flexible. At the nanoscale, interactions between nanoparticles (NPs), such as van der Waals forces, electrostatic forces, and hydration forces, influence their mechanical behavior. The DLVO, JKR, and DMT theories attempt to explain these interactions, describing adhesion, aggregation, and surface energy effects. However, there is ongoing debate about whether continuum mechanics can accurately describe nanoparticle behavior at such small scales **(Bhosale et *al*., 2024).**

5.2. Thermal properties

Nanoparticles (NPs) transfer heat mainly through electron and photon conduction. Their small size increases surface-to-volume ratio, enhancing thermal conductivity. In nanofluids, Brownian motion further improves heat transfer, as seen in Cu NPs boosting ethylene glycol's conductivity by 40%.

NPs also have higher heat capacity and lower melting points due to surface energy effects; for example, 3 nm gold NPs melt 300°C lower than bulk gold. Bimetallic NPs offer greater thermal stability than monometallic ones **(Bhosale et *al*., 2024).**

5.3. Electronic and optical properties

Metallic and semiconductor nanoparticles (NPs) exhibit unique optical properties due to quantum confinement and localized surface plasmon resonance (LSPR). LSPR causes strong UV-visible absorption, influenced by NP size, shape, and surrounding environment. Smaller NPs absorb at shorter wavelengths, while larger or oblate-shaped NPs shift absorption toward the red spectrum.

The optical behavior of NPs also depends on their surroundings, NPs on substrates show red shifts compared to free NPs. Additionally, biogenic NPs, synthesized from plant extracts, display enhanced optical and photocatalytic properties due to their smaller size and better crystallinity, improving applications in photodegradation and energy-related fields **(Bhosale et *al*., 2024).**

6. Toxicokinetic of nanoparticles

6.1. Important Routes of Exposure

Nanoparticles enter the body mainly through inhalation, skin contact, and ingestion.

- **Skin:** Exposure occurs through cosmetics, topical drugs, or occupational

contact. Penetration depends on skin condition; damaged or flexed skin allows deeper entry. Once absorbed, nanoparticles can reach the lymphatic system, bloodstream, and even nerves.

- **Respiratory Tract:** Inhaled nanoparticles deposit throughout the lungs based on size. They can cross into the blood and lymph, reaching organs like the heart, brain, and spleen. They may trigger inflammation, oxidative stress, and systemic effects, especially in vulnerable individuals.
- **Gastrointestinal Tract:** Exposure occurs via ingestion of contaminated food, water, or drugs. Ingested nanoparticles may be more toxic than larger particles, affecting organs like the liver and kidneys

(Forbe et *al*., 2011).

6.2. Distribution

After intravenous injection, nanoparticles distribute to organs like the colon, lungs, bone marrow, liver, spleen, and lymphatic system. Clearance from the bloodstream occurs rapidly, mainly via hepatic and splenic macrophages, and is influenced by nanoparticle size and surface properties. Inhaled nanoparticles accumulate in the lungs, liver, heart, and kidneys, with clearance in the alveoli primarily through macrophage phagocytosis, supported by physical processes like mucociliary movement, translocation, and lymphatic drainage. Orally ingested nanoparticles are found in the kidneys, liver, spleen, lungs, brain, and GI tract **(Forbe et *al*., 2011).**

6.3. Metabolism

Nanoparticles in the GI tract can be absorbed into the bloodstream and then distributed systemically. Some are rapidly eliminated in feces and urine, while others may accumulate in the liver due to first-pass metabolism. The rate and location of metabolism depend on absorption efficiency and nanoparticle characteristics **(Forbe et *al*., 2011).**

6.4. Excretion

Nanoparticles are excreted mainly via the kidneys or the liver/bile duct. Surface chemistry plays a major role: for example, hydroxyl-functionalized carbon nanotubes accumulate in the liver and kidneys and are cleared in urine within 18 days, while ammonium-

functionalized nanotubes show faster renal excretion and no liver uptake. Some nanoparticles, like quantum dots (QDs), may not be excreted unless they are smaller than 5.5 nm and cysteine-coated, in which case they can be eliminated through urine. Long-term behavior of non-excreted nanoparticles remains uncertain **(Forbe et *al*., 2011).**

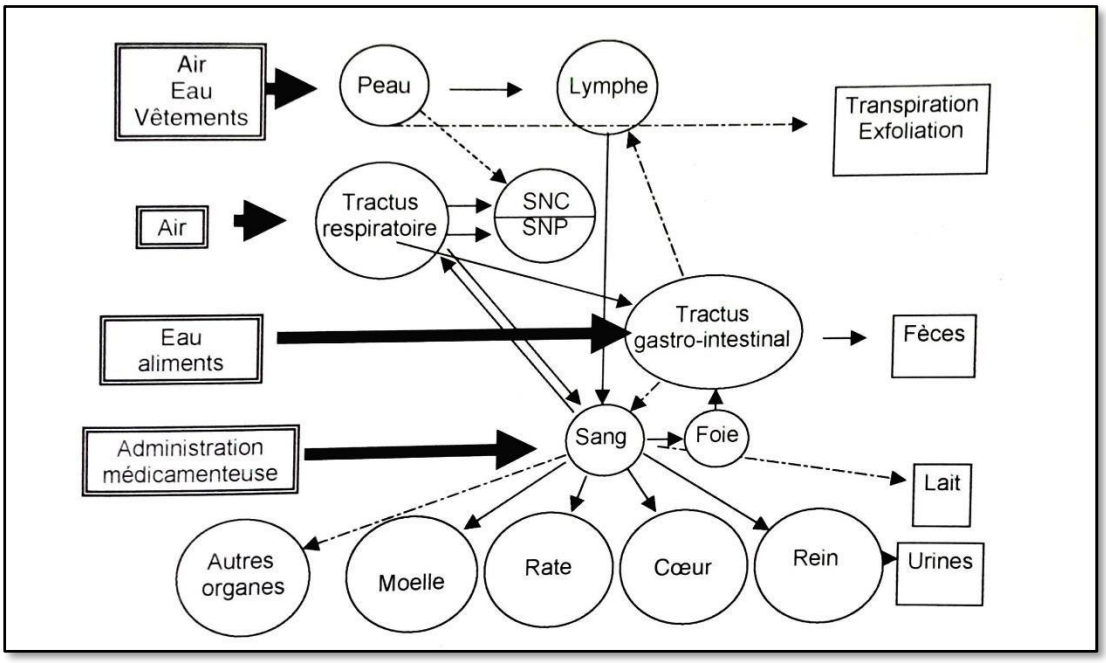


Figure 4: Biodistribution of nanoparticles in the body **(Viala & Botta, 2005)**.

7. Nanotoxicity

Nanotoxicity refers to the potential harmful effects of nanomaterials on biological tissues, posing significant health risks, especially in applications like drug delivery, diagnostics, vaccines, and gene therapy. Several factors influence nanotoxicity, including particle size, dose regimen, route of exposure, degree of aggregation, and surface chemistry. Smaller nanoparticles (<50 nm) tend to exhibit greater toxicity due to their increased penetrability, reactivity, and ability to evade immune clearance. Additionally, higher doses and certain exposure routes, such as inhalation or intravenous administration, can exacerbate toxic effects on organs like the lungs, liver, kidneys, heart, and spleen. Aggregated nanoparticles may also induce greater toxicity than their de-aggregated count erparts. However, surface functionalization with agents like sodium citrate or PVP can reduce toxicity by limiting metal ion leaching and immune activation. Understanding these factors is crucial for designing safer nanomaterials and mitigating adverse health effects **(Thu et *al*., 2023).**

8. Impact of NPs on Biological Systems

The increasing use of NPs raises concerns about their potential toxicological and hazardous effects on human health and the environment. These particles can be released during production, use, recycling, and disposal, persisting in air, water, soil, and biological systems. They can enter the human or animal body through the skin, ingestion, or inhalation and subsequently spread to different organs. Exposure to NPs has been linked to the activation of proinflammatory cytokines and chemokines, disrupting immune system balance and increasing the risk of autoimmune, allergic, or neoplastic diseases. Furthermore, ultrafine particles have been associated with pulmonary, cardiac, and central nervous system disorders. In plants, NPs can penetrate cells and cause harmful effects, such as root growth inhibition, as observed with ZnO and Al NPs **(Joudeh & Linke, 2022).**

Chapter 02:

Toxicological impact of Nanoparticles on renal mitochondria

1. Definitions and fundamental concepts

1.1. Nickel (Ni)

1.1.1. Definition

Nickel is a silver-white metal with shiny appearance and siderophilic properties that facilitate the formation of nickel-iron alloys. It exists in various forms, including soluble salts (chloride, nitrate, sulfate) and poorly water-soluble compounds (metallic nickel, nickel sulfides, and nickel oxides). Nickel carbonyl is a volatile liquid that decomposes into carbon monoxide and nickel **(Barceloux & Barceloux, 1999).**

1.1.2. Nickel in Soil: Occurrence and Bioavailability

Nickel is a naturally occurring metallic element, ranking as the 24th most abundant in the Earth's crust. Its presence in soils is primarily attributed to the weathering of parent materials, especially ultramafic rocks like serpentinites, which are rich in iron and phosphate-bearing minerals. Soil nickel content varies significantly, ranging from 0.2 to 450 mg/kg, with a global average estimated between 70 and 85 mg/kg. In the environment, nickel exists predominantly as the divalent cation Ni^{2+}, which is the form readily absorbed by plants. However, its bioavailability in soils is influenced by factors such as pH, organic matter content, and soil moisture, affecting its uptake by plants.**(Rabinovich et *al.*, 2024)**

1.1.3. Sources, Uptake, and Health Risks of Nickel

Nickel exposure mainly comes from industrial processes like nickel-plating, stainless-steel production, anticorrosion coatings, catalysis, nickel-cadmium batteries, pigments, and coins. Nickel carbonyl, a toxic and carcinogenic compound, may also be present in tobacco smoke.

Soluble nickel salts are poorly absorbed but are mostly bound to plasma proteins in the blood and are eliminated quickly, mainly through urine. Nickel carbonyl, however, is well absorbed through inhalation or skin contact and can cross the placental barrier.

Nickel is an essential trace element but can become toxic at high doses, causing respiratory irritation, skin sensitization, immune disturbances, kidney damage, and potentially cancers (lungs, sinuses, larynx, stomach).

Occupational exposure limits vary by compound. Normal nickel levels are ≤4 µg/L in blood and

≤2–10 µg/L in urine. The WHO sets strict limits for air and drinking water concentrations. Treatment of nickel poisoning is mainly symptomatic, with chelators used in serious cases,

especially involving nickel carbonyl. **(Viala & Botta, 2005)**



Figure 5: Raw Nickel Sample **(MAT, 2023)**

1.1.4. Physical Properties

Atomic number	28
Atomic weight	58.69
Melting point, ℃	1,455
Boiling point, ℃	2,730
Relative density, 25℃	8.9
Volume increase on melting, %	4.5
Heat of fusion at m.p, J/g	302
Heat of sublimation at 25℃, J/g	7,317
Heat of vaporization, J/g	6,375
Thermal conductivity (0 – 100 C̊), W m^{-1} k^{-1}	88.5
Heat capacity (0 – 100℃), J g^{-1} k^{-1}	0.452
Electrical resistivity at 20°C, μΩ/cm	6.9

Table 01: Physical Properties of nickel **(Habashi, 2013)**

1.2. Nickel Dioxide (NiO_2)

Nickel Dioxide (NiO_2) is a less common and less stable oxide of nickel compared to the well-known Nickel (II) Oxide (NiO). While NiO features nickel in the +2 oxidation state and crystallizes in a stable cubic lattice, NiO_2 contains nickel in the +4 oxidation state, giving it significantly higher oxidative potential. NiO_2 typically appears as a black or dark brown crystalline solid and is of particular interest in electrochemical

applications such as battery cathodes and advanced catalysis, where high-valent nickel species are required.

In contrast, NiO has been widely studied for its diverse functional properties including semiconducting behavior, electrochemical durability, and its role in catalysis, gas sensing, and biosensing. At the nanoscale, NiO exhibits enhanced characteristics due to surface and quantum size effects, making nanostructured NiO valuable in fields like glucose biosensing and photocatalysis **(El-Kemary et *al.*, 2013)**. Although NiO_2 remains less explored, especially in biological systems, its strong oxidative nature and redox activity make it a candidate of growing interest in toxicological and energy research.

1.3. Nephrotoxicity of Nanoparticles

1.3.1. Definition

Nephrotoxicity refers to the rapid decline in kidney function caused by exposure to medications and chemicals. It is also characterized as an adverse effect resulting from substances that impair renal function. These harmful substances may include fungi and molds, cancer treatments, antibiotics, heavy metals like arsenic, lead, and mercury, as well as illicit drugs **(B.Sc, 2022)**.

1.3.2. Biomarkers of Nephrotoxicity

Nephrotoxicity biomarkers are crucial for detecting early kidney damage, as traditional markers like blood urea and serum creatinine have low sensitivity. Urinary proteins serve as key indicators, with high-molecular-weight proteins (e.g., albumin, transferrin, immunoglobulin G) signaling glomerular dysfunction and low-molecular-weight proteins (e.g., Cystatin C, KIM-1, β2- microglobulin) indicating tubular damage. KIM-1 is highly upregulated during nephrotoxic injury, while NGAL is linked to renal inflammation. Cystatin C provides a more precise measure of GFR decline than creatinine. IL-18 contributes to renal fibrosis and acute kidney injury, while Vitronectin (VTN) and Integrins (ITNs) influence renal repair and fibrosis. These biomarkers,

detected in urine and blood, offer valuable insight into drug-induced nephrotoxicity, acute kidney injury (AKI), and chronic kidney disease (CKD) progression, aiding in diagnosis and treatment **(Al-Naimi et *al.*, 2019).**

1.3.3. The implication of nephrotoxicity

1.3.3.1. Distribution of nanoparticles to kidney

Nanoparticles (NPs) are distributed to the kidneys through systemic circulation via the renal artery, where blood flow and vascular permeability influence their movement within renal tissues. Their distribution depends on factors such as NP size, surface properties, and kidney functionality. In healthy kidneys, NPs with specific surface modifications, like maleimide end-groups, may exhibit enhanced distribution. In contrast, renal impairment can alter NP distribution, leading to increased presence in the renal medulla due to changes in vascular permeability **(Xin et *al*., 2022)**

1.3.3.2. Accumulation in renal tissues and filtration pathways

Nanoparticles (NPs) can accumulate in renal tissues depending on the kidney's filtration processes. The glomerular filtration barrier (GFB) generally prevents particles larger than 6–8 nanometers from passing into the urine. However, some studies suggest that larger NPs may bypass this barrier, either through alternative filtration pathways or temporary disruptions in the GFB. After crossing the GFB, NPs can be reabsorbed or processed within renal tubules, leading to their accumulation in kidney tissues, which is important for both therapeutic applications and potential nephrotoxicity **(Adhipandito et *al*., 2021).**

1.4. Bioenergetics

Bioenergetics refers to the interconnected energy-transducing pathways within mitochondria that are responsible for maintaining the cell's phosphorylation potential. These pathways play a critical role in assessing mitochondrial function or dysfunction. By measuring different aspects of bioenergetics, researchers can gain valuable insights into the overall health and state of the mitochondrial population being studied. Bioenergetics has become a key diagnostic tool in the fields of biomedicine and life sciences, enabling scientists to evaluate mitochondrial activity and dysfunction. The understanding of bioenergetics has also facilitated the development of various technologies that explore mitochondrial function, making this specialized field more accessible across diverse scientific disciplines **(Mailloux et *al*., 2023).**

1.5. Mitochondrial Dysfunction: Its Role in Renal Pathophysiology

1.5.1. Definition

Mitochondria, often called the "power plants of the cell" do not produce energy but convert

it from one form to another. They are small organelles, typically 1–2 µm in length, with a double membrane, the inner one forming folds called cristae. Found near ATP consumption sites, mitochondria are associated with the cytoskeleton and vary greatly in number, shape, and size depending on the cell type and its activity. They form a dynamic network (chondriome) that can move, fuse, divide, and change shape. Mitochondria occupy about 15–20% of a cell's volume, and their number is regulated by the cell's metabolic needs **(Bassaglia, 2004)**. Mitochondria are intracellular organelles responsible for generating the majority of the body's ATP, serving as the primary energy source for eukaryotic cells. They originate from endosymbiotic prokaryotes and are essential for cellular energy production.

Mitochondrial dysfunction is implicated in various mitochondrial diseases, particularly neuromuscular disorders, which can manifest in both children and adults. Additionally, it plays a significant role in critical illnesses and may contribute to multi-organ dysfunction syndrome (MODS), especially in severe sepsis.

Research on mitochondrial dysfunction in organs prone to failure in critical care conditions; such as the liver, kidneys, heart, lungs, intestines, and brain, primarily comes from animal models. However, there is currently no well-established therapeutic approach to effectively address acquired mitochondrial dysfunction **(Bassaglia, 2004)**.

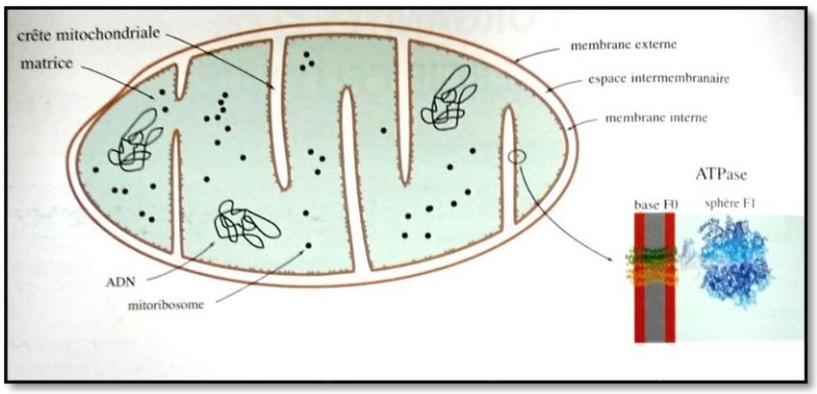


Figure 6: Structural Organization of a Mitochondrion **(Bassaglia, 2004).**

1.5.2. Role of Mitochondria:

Mitochondria play a crucial role in cellular function and survival by:

- Generating ATP, the primary energy source.
- Regulating apoptosis, ensuring controlled cell death.
- Producing reactive oxygen species (ROS) for cell signaling.

- Maintaining calcium homeostasis for cellular stability.
- Synthesizing biomolecules, including heme and iron-sulfur clusters.
- Participating in hormone metabolism, influencing cortisol and estrogen activity.
- Supporting thermoregulation, contributing to heat production.

These functions highlight mitochondria's vital role in cellular energy, metabolism, and homeostasis
(Nickson, 2019).

1.5.3. Mitochondrial Function in ATP Synthesis

Mitochondria are double-membraned organelles responsible for producing most of the cell's ATP through oxidative phosphorylation. Their inner membrane forms cristae, increasing surface area for energy reactions, while the matrix contains mitochondrial DNA and metabolic enzymes. Mitochondria break down pyruvate and fatty acids into acetyl-CoA, which enters the citric acid cycle, generating NADH and $FADH_2$. These molecules fuel the electron transport chain in the inner membrane, creating a proton gradient that drives ATP synthesis. Oxygen acts as the final electron acceptor, completing the process of energy production **(Cooper & François, 1999).**

1.5.4. Role of Renal Mitochondria in Kidney Function

Renal mitochondria are essential for maintaining kidney function, primarily through ATP production via oxidative phosphorylation. This energy supports critical renal processes such as filtration, reabsorption, and secretion. Additionally, mitochondria regulate reactive oxygen species (ROS) levels, calcium homeostasis, and apoptosis, all vital for cellular health. Mitochondrial dysfunction, characterized by decreased ATP production and increased ROS, contributes to the development and progression of acute kidney injury (AKI) and chronic kidney disease (CKD). Therefore, maintaining mitochondrial health is crucial for proper kidney function and overall renal health. (*The Roles of Mitochondrial to Chronic Kidney Disease*, n.d.)

1.6. Oxidative stress

1.6.1. Definition

Oxidative stress refers to an imbalance favoring oxidants over antioxidants, resulting in

altered redox signaling and potential molecular damage.

The antioxidant defense mainly relies on endogenous enzymes, while external compounds play a lesser role. Such an imbalance disturbs the normal redox state, activating cellular stress responses. It encompasses both normal physiological roles "oxidative eustress" and harmful excesses "oxidative distress".

This condition can damage various biomolecules, including proteins, lipids, carbohydrates, and DNA **(Sies, 2020).**

1.6.2. Oxidative Stress and Mitochondrial Impairment in Renal Pathologies

Mitochondria are particularly susceptible to oxidative stress, as the respiratory chain is a major source of reactive oxygen species (ROS), with 2 to 4% of oxygen being incompletely reduced. This leads to damage within key mitochondrial components: the proteins of the respiratory complexes in the inner membrane are inhibited, reducing energy production; mitochondrial DNA, lacking histones and introns, is highly vulnerable and prone to mutations due to its limited repair capacity. These disruptions impair the synthesis of membrane protein complexes and oxidative phosphorylation, which further increases ROS production and contributes to a cycle of mitochondrial dysfunction **(Descamps, 2008).**

The nephron, the kidney's functional unit, is composed of various cell types, including endothelial, mesangial, podocytes, and epithelial cells. Mitochondrial damage in these cells is linked to renal conditions such as tubulointerstitial injury, glomerular hypertrophy, and nephrotic syndromes, potentially increasing mortality risk. Chronic kidney disease (CKD) involves progressive nephron loss, inflammation, fibrosis, and reduced regenerative capacity, and is diagnosed when kidney damage persists for over three months. CKD classification is based on estimated glomerular filtration rate and albuminuria levels and often results in complications such as atherosclerosis and hypertension. Oxidative stress, through an imbalance between ROS and antioxidant defenses, contributes to disease progression and vascular damage. Furthermore, mitochondrial-targeted therapies are being explored to maintain mitochondrial function, enhance antioxidant defenses,

support energy metabolism, and regulate mitophagy and dynamics in CKD management **(Ho & Shirakawa, 2023).**

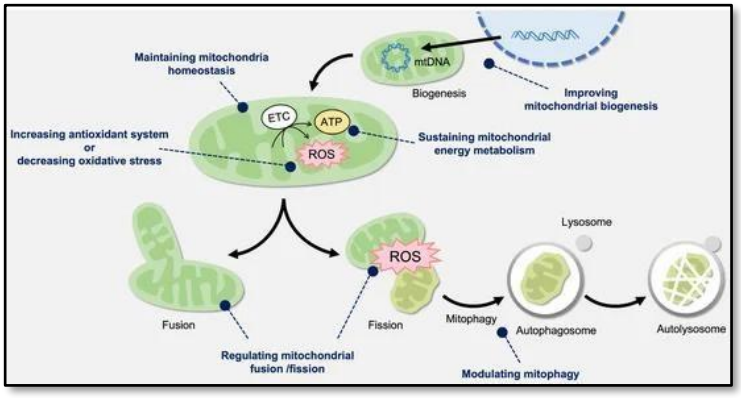


Figure 7: Mitochondrial Dynamics and Targets for Oxidative Damage **(Ho & Shirakawa, 2023).**

2. Mechanisms of Nanoparticle-Induced Mitochondrial Toxicity

2.1. Internalization of Nanoparticles by Renal Cells

Nickel oxide nanoparticles (NiO-NPs) can accumulate in renal tissue due to their nanoscale size, allowing them to bypass biological barriers and deposit in organs like the kidneys. Once inside renal tubular cells, NiO-NPs may interact with intracellular structures including mitochondria, initiating cytotoxic effects. Researchers have shown that NiO-NP exposure can provoke inflammatory responses, histological changes, and biochemical disruptions in kidney tissues, all of which indicate their strong nephrotoxic potential **(Capasso et *al.*, 2014)**.

2.2. Effects on Mitochondrial Membrane Potential (Δψm)

NiO-NPs disrupt mitochondrial membrane potential (Δψm), which is essential for maintaining ATP synthesis through oxidative phosphorylation. The depolarization of this membrane potential impairs mitochondrial respiration and energy metabolism. Experimental data from various cell models confirm that NiO-NP exposure results in a dose-dependent decrease in Δψm, leading to cellular energy deficits and mitochondrial failure **(Patrón-Romero et *al.*, 2022)**.

2.3. Induction of Mitochondrial Permeability Transition Pore (mPTP)

NiO-NPs have also been shown to activate mitochondrial apoptotic pathways. Mitochondrial membrane damage leads to the release of cytochrome c into the cytoplasm, which activates

downstream caspases like caspase-3. This process, regulated by the Bcl-2 family of proteins, drives programmed cell death and contributes to tissue damage in the kidneys **(Lozano et *al*., 2020).**

2.4. Damage to Mitochondrial DNA (mtDNA)

The elevated oxidative stress caused by NiO-NPs also contributes to mitochondrial DNA (mtDNA) damage. Damage to mtDNA affects gene expression and replication necessary for mitochondrial function. Studies involving metallic nanoparticles have demonstrated increased markers of oxidative DNA damage, such as 8-OHdG, and show that this impairment is linked with mitochondrial and cellular dysfunction in renal tissue **(Abudayyak et *al*., 2017).**

2.5. Impairment of Mitochondrial Dynamics

Nickel oxide nanoparticles (NiO-NPs) disrupt mitochondrial dynamics by altering the delicate equilibrium between fusion and fission processes. This balance is crucial for maintaining mitochondrial repair mechanisms and turnover. When disturbed by nanoparticle exposure, it leads to abnormal mitochondrial structure, hindered biogenesis, and a decreased ability of the organelle to adapt under stress conditions, ultimately contributing to cellular damage **(Luo et *al*., 2024)**.

3. Autophagy and Mitophagy in Response to Nanoparticle Exposure

3.1. Role of Autophagy in Nanoparticle Detoxification

Autophagy plays a vital role in cellular defense by maintaining homeostasis through the degradation and recycling of damaged organelles and proteins. Nanoparticle (NP) exposure has been found to influence autophagic activity, which may either protect cells or contribute to toxicity, depending on the exposure conditions. In the context of renal cells, certain nanoparticles have been reported to stimulate autophagy, facilitating cellular detoxification and offering protection against kidney toxicity. Research indicates that enhanced autophagic flux in response to nanoparticle exposure can help alleviate oxidative stress and minimize tissue damage in the kidneys **(Florance et *al*., 2024)**.

3.2. Mitochondrial Quality Control via Mitophagy

Mitophagy, the targeted autophagic clearance of damaged mitochondria, is a critical component of mitochondrial quality control, particularly in metabolically active organs such as the kidneys. This mechanism facilitates the elimination of dysfunctional mitochondria, thereby limiting reactive oxygen species (ROS) accumulation and preserving cellular

integrity. Under nanoparticle exposure, mitophagy may be upregulated as an adaptive response to remove mitochondria impaired by oxidative stress. Emerging evidence suggests that stimulation of mitophagic pathways can mitigate mitochondrial dysfunction and attenuate renal injury triggered by nanoparticle-induced cellular stress **(Yang et *al*., 2024)**.

3.3. Dysregulation of Mitophagy in Kidney Cells

Mitophagy dysregulation in renal cells following nanoparticle exposure can lead to harmful effects. When the process fails to eliminate damaged mitochondria efficiently, dysfunctional organelles accumulate, resulting in elevated ROS levels, reduced ATP production, and the triggering of pro-apoptotic pathways. This imbalance intensifies oxidative stress in the kidneys and may contribute to the development of chronic renal dysfunction. Research indicates that nanoparticles such as nickel oxide (NiO) NPs can disrupt mitophagy signaling by interfering with critical regulators like PINK1 and Parkin, thereby impairing mitochondrial quality control and heightening cellular stress in kidney tissues **(Yin et *al*., 2024)**.

4. Techniques for Assessing Mitochondrial Impairment

4.1. In Vivo vs. In Vitro Models in Renal Nanotoxicology

In renal nanotoxicology, in vitro models rely on cultured kidney cell lines or primary renal cells to evaluate nanoparticle (NP) toxicity in a controlled environment. These models offer several benefits, including cost-effectiveness, rapid analysis, high reproducibility, and the capacity to assess various concentrations and nanoparticle formulations. They are particularly useful for preliminary toxicity evaluations and exploring underlying mechanisms. However, they do not replicate the full physiological complexity of living organisms, such as blood circulation, metabolic activity, and immune system interactions. Conversely, in vivo models, typically involving rodents, are crucial for examining the systemic effects of NPs, including their distribution, renal elimination, long-term toxicity, and accumulation in specific organs. These models better reflect real-life exposure and capture complex biological interactions, offering a more comprehensive view of NP toxicity. Nonetheless, in vivo studies are more resource-intensive, ethically regulated, and may be limited by species-specific differences that reduce their direct relevance to human health **(Gornati et *al*., 2009)**.

4.2. Electron Microscopy and Mitochondrial Imaging

Electron microscopy (EM) remains a critical technique for the high-resolution visualization

of mitochondrial ultrastructure, enabling precise analysis of features such as cristae organization, membrane continuity, and organelle interactions. Accurate assessment of these parameters requires rigorously standardized protocols, including proper fixation, sectioning, and imaging conditions to preserve mitochondrial morphology. Recent insights emphasize the necessity of quantitative analysis in EM imaging to evaluate mitochondrial health and detect subtle structural alterations associated with pathological states, including nanoparticle-induced toxicity. Moreover, the integration of EM with complementary imaging techniques and biochemical assays enhances the reliability and depth of mitochondrial assessments, contributing to a more comprehensive understanding of mitochondrial dynamics in renal nanotoxicology **(Salzillo et *al*., 2023)**.

4.3. Assays for Mitochondrial Function

The evaluation of mitochondrial function is a critical component in assessing the cellular impact of nanoparticle (NP) exposure, particularly in the context of energy metabolism and cell viability. One commonly employed method is the JC-1 assay, which provides insight into mitochondrial membrane potential ($\Delta\Psi m$) a key marker of mitochondrial integrity. The JC-1 dye preferentially accumulates within mitochondria in a manner dependent on membrane polarization. In healthy mitochondria, the dye aggregates and emits red fluorescence, whereas in depolarized or dysfunctional mitochondria, it remains in monomeric form, producing green fluorescence. This ratiometric shift from red to green serves as a sensitive indicator of early mitochondrial depolarization, enabling researchers to detect sublethal mitochondrial dysfunction before the onset of overt cytotoxicity **(Smiley et *al*., 1991).**

In addition to membrane potential measurements, quantifying intracellular adenosine triphosphate (ATP) levels offers complementary insights into mitochondrial performance, particularly with respect to cellular energy production. As ATP is the primary energy currency of the cell, a reduction in its levels is indicative of mitochondrial impairment and altered metabolic activity. ATP-based assays are highly sensitive and well-suited for high-throughput applications, making them especially valuable in nanotoxicology studies aimed at detecting early bioenergetic disturbances induced by nanoparticle exposure **(Chang et *al*., 2024)**.

The measurement of oxygen consumption rate (OCR) is a pivotal technique for evaluating mitochondrial respiratory function in live cells. Utilizing instruments such as the Seahorse XF Analyzer, researchers can obtain real-time assessments of various parameters, including

basal respiration, ATP-linked respiration, maximal respiratory capacity, and spare respiratory capacity. These measurements provide a comprehensive bioenergetic profile of cells, enabling the elucidation of mitochondrial oxidative phosphorylation efficiency and the impact of external factors, such as nanoparticle exposure, on cellular metabolism **(Divakaruni et *al*., 2014).**

Part II

Materials, methods & experimental study

1. Material and methods

1.1. Material

1.1.1. Biological material

The study was conducted in the laboratories of Larbi Tébessi University in Tébessa, using 18 white male Wistar rats (Rattus norvegicus), obtained from the Pasteur Institute in Algiers. The animals were approximately nine weeks old, with body weights ranging from 170 to 300 grams. As members of the rodent family, Wistar rats are commonly used in laboratory research due to their well-characterized biological and physiological traits.



Figure 8: Animal material **(personal picture)**

1.1.2. Chemical material

In this study, nickel dioxide (NiO_2) was used for the treatment of rats, administered in a distilled water solution at two doses: 5 mg/kg/day and 15 mg/kg/day.

1.1.3. Animal Diet

Throughout the experimental period, the animals were fed a nutritionally balanced commercial pellet diet formulated to meet the standard dietary requirements of laboratory rats. The composition of the feed was as follows: corn (62%), crude protein (22%), crude fat (1.6%), crude fiber (1.0%), minerals (1.0%), and vitamins (1.0%). This standardized diet was maintained consistently to ensure uniform nutritional intake across all groups and to eliminate potential dietary variables that could influence the effects of nickel dioxide

nanoparticles (NiO_2 NPs) on renal mitochondrial function.

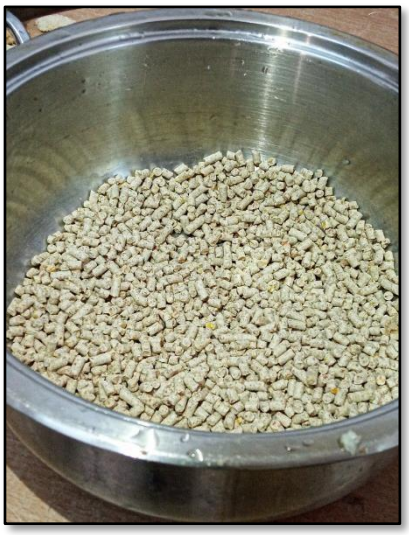


Figure 9: Rat Food "Croquettes" **(personal picture)**

1.2. Methodology

1.2.1. Subdivision and processing

The rats were randomly divided into three groups, each consisting of six (06) animals. A 20-day acclimatization period was conducted in the animal facility of the Department of Biology, Faculty of Science, University of Tebessa. During this period, environmental conditions were maintained at a temperature of 23 ± 2 °C, with a natural 12-hour light/dark cycle and a relative humidity of approximately 60%. The animals were housed in polyethylene cages, each containing six (06) rats, with wood shavings used as bedding. Cages were cleaned and bedding was replaced every two days throughout the experimental period.



Figure 10: Rat distribution **(personal picture).**

1.2.2. Justification for Dose Selection

In this study, two oral doses of nickel dioxide nanoparticles (NiO_2 NPs), 5 mg/kg/day and 15 mg/kg/day, were administered chronically to evaluate their potential nephrotoxic effects. The selection of these doses was guided by prior research demonstrating the organ-specific accumulation and toxic potential of metal oxide nanoparticles, particularly in the kidneys, as shown in the study by **(Areecheewakul et *al.*, 2020)**. Their findings highlight the vulnerability of renal tissue to oxidative stress and mitochondrial dysfunction induced by nanoparticle exposure. Furthermore, the study by **(Alhazmi et *al.*, 2024)** confirmed the nephrotoxicity of nickel oxide nanoparticles and their impact on renal antioxidant defense systems. These dose levels were thus selected to represent environmentally and occupationally relevant exposures, enabling the assessment of dose-dependent mitochondrial alterations in renal tissue.

1.2.3. Preparation of the solution

For the preparation of the solutions, 5 mg and 15 mg of powdered nickel dioxide (NiO_2) were each dissolved in 100 mL of distilled water in separate vials and thoroughly mixed using a mechanical agitator. The solutions were then administered to the rats orally.

1.2.4. Weight measurement

Body weight measurements were consistently carried out on the rats throughout both the acclimatization and treatment periods to assess any physiological changes. During the acclimatization phase, weight monitoring was conducted to evaluate possible variations related to environmental or dietary factors. During the treatment phase, it served to track potential effects induced by xenobiotic exposure. All measurements were performed using a 500 g precision balance.

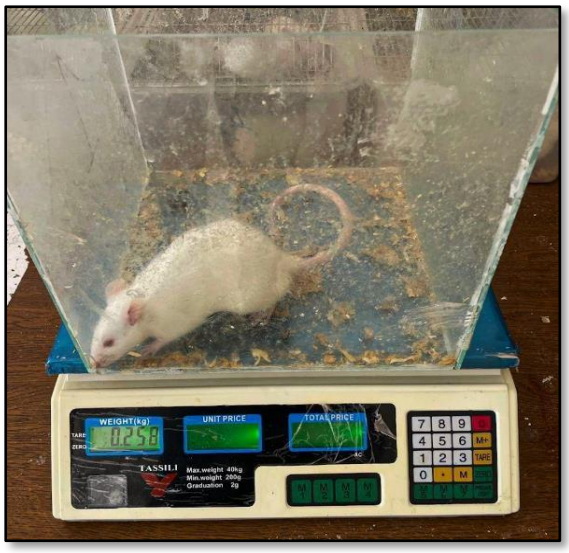


Figure 11: Weight measurement **(personal picture).**

1.2.5. Treatment of rats

The experiment was divided into three groups as follows:

Lot 1: Consisted of 6 rats serving as the control group, which did not undergo any treatment.

Lot 2: Consisted of 6 rats treated with nickel dioxide (NiO_2) at a dose of 5 mg/kg, administered orally.

Lot 3: Consisted of 6 rats treated with nickel dioxide (NiO_2) at a dose of 15 mg/kg, administered orally.

1.2.6. Sacrifice and taking of samples

A. Animal sacrifices

At the conclusion of the treatment period, the rats were fasted overnight and subsequently sacrificed by decapitation.



Figure 12: sacrifices of rats **(personal picture).**

B. Sacrifice and extraction of the kidneys:

The kidneys were promptly harvested following dissection and rinsed in a 0.9% sodium chloride (NaCl) solution. The tissue samples were then stored at -80°C for subsequent analysis of biochemical parameters, including proteins and lipids, as well as oxidative stress markers such as GSH, GST, GPx, CAT, and MDA.



Figure 13: sacrifice and kidney removal **(personal picture).**

C. Estimate of relative kidney weight:

The relative kidney weight (RKW) was calculated as a ratio of kidney weight to total body weight (g/100 g body weight) using the following formula:

$$\text{PRC (g/100g de PT)} = \text{PC/PT} \times 100$$

PC: weight of the kidney

(g). PT: total weight of rat

(g).

PRC: relative weight of kidneys (g)

D. Preparation of mitochondrial suspensions

Kidney tissue homogenates were prepared by homogenizing 200 mg of renal tissue in 4 mL of isolation buffer (210 mM mannitol, 70 mM sucrose, 1 mM Tris-HCl, 1 mM EDTA, pH 7.5) using a Potter Elvehjem homogenizer. The homogenate was subjected to differential centrifugation at 4 °C: first at 1,300 × g for 3 minutes, followed by centrifugation of the resulting supernatant at 10,000 × g for 10 minutes to sediment the mitochondria. The supernatant was discarded, and the mitochondrial pellet containing highly purified mitochondria was carefully collected and washed twice with the isolation buffer.

Mitochondrial oxygen consumption was measured according to the method described by **(Rouabhi et *al.*, 2015)** using a Clark-type polarographic oxygen electrode (HANSATECH), mounted within a DW1/AD electrode chamber and connected to the Oxygraph+ electrode control unit. Following the experimental protocol, 1 mg of purified renal mitochondria was suspended in 1 mL of respiration buffer (0.23 M mannitol, 0.07 M sucrose, 20 mM Tris–HCl, pH 7.4, 1 mM EDTA, 5 mM phosphate, 4 mM $MgCl_2$) and transferred to the incubation chamber. Oxygen consumption was continuously recorded, with data displayed on a computer connected to the oxygraph system.

After an initial 4-minute recording, 200 µL of ADP (1 mM) was added to stimulate state 3 respiration. After 10 minutes of recording, 200 µL of succinate (10 mM) was introduced to support complex II driven respiration. Isolated mitochondria were maintained on ice and used within 4 hours of isolation. Protein content was determined using the Bradford assay **(Bradford, 1976)** with bovine serum albumin as the standard.

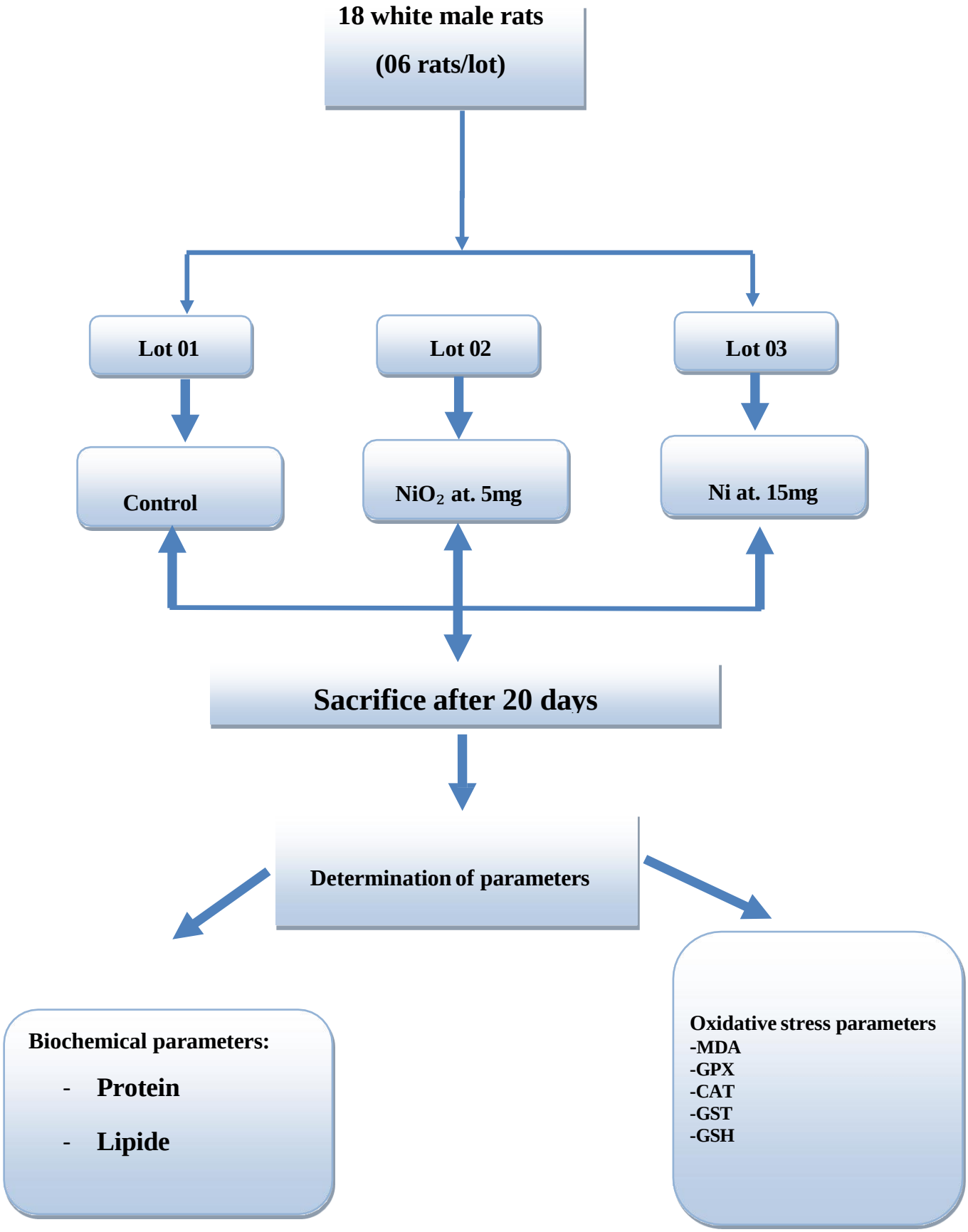


Figure 14: Summary Diagram of the Experimental Protocol

1.3. Methods of dosage

The extraction of various metabolites was carried out following the procedure described by **(Shibko et *al*.,1966),** with the main steps illustrated in Figure 06. Control and treated tissue samples were homogenized using a tissue grinder in 20% trichloroacetic acid (TCA), at a ratio of 200 mg of tissue per 1 mL of TCA. The homogenates were centrifuged at 5000 rpm for 10 minutes at 4 °C. The resulting supernatant was discarded, and the remaining pellet (Pellet I) was resuspended in 1 mL of an ether/chloroform mixture (1:1, v/v), followed by a second centrifugation under the same conditions. The resulting supernatant (Supernatant II) was used for lipid quantification according to the method of **(Goldsworthy et *al*.,1972),** while the final pellet (Pellet II) was dissolved in 0.1 N NaOH and used for protein quantification using the method of **(Bradford, 1976)**.

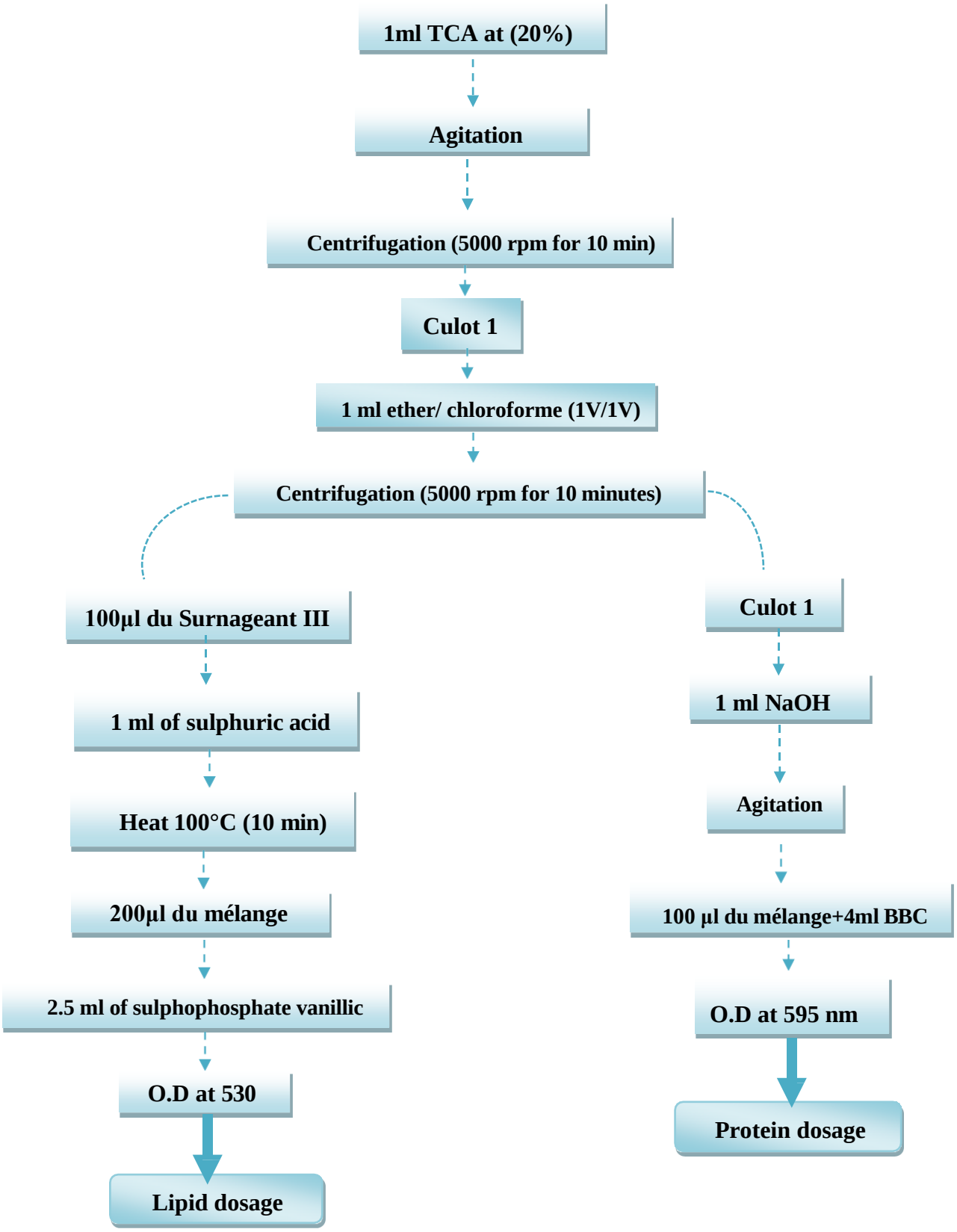


Figure 15: Extraction methods and assay of major biochemical constituents (lipids, proteins.)

1.3.1. Determination of biochemical parameters

A. Protein dosage

The assay of proteins was carried out according to the method of **(Bradford, 1976)**, which uses Coomassie Brilliant Blue (CBB) as the reagent. This dye binds to proteins, resulting in a blue coloration proportional to the protein concentration. Bovine Serum Albumin (BSA) was used as the standard. The calibration curve was established from a stock solution of BSA at 1 mg/mL. The CBB reagent (stable for about 21 days at 4 °C) was prepared as follows:

- 100 mg of CBB dissolved in 50 mL of ethanol, with agitation for two hours.
- 100 mL of orthophosphoric acid was then added, and the volume was adjusted to 1000 mL with distilled water.
- The protein assay was performed using an aliquot of 100 µL.
- The absorbance was measured using a spectrophotometer at a wavelength of 595 nm.

B. Lipid dosage

Total lipids were determined according to the method of **(Goldsworthy et *al.*, 1972)**, using the sulfo-phospho-vanillin reagent, prepared from:

- 0.38 g of vanillin
- 195 mL of 85% orthophosphoric acid
- 55 mL of distilled water

A stock lipid solution at 2.5 mg/mL was used as the

standard. The assay was performed as follows:

- 1 mL of concentrated sulfuric acid (98%) was added to each sample tube.
- After mixing, the tubes were heated in a water bath at 100 °C for 10 minutes.
- Then, 200 µL from each tube was transferred to a new tube, and 2.5 mL of sulfo-phospho- vanillin reagent was added.
- The absorbance was measured after 30 minutes in the dark at a wavelength of 530 nm using a spectrophotometer.

1.3.2. Oxidative stress parameters

This includes enzymatic and non-enzymatic parameters.

1.3.2.1. Non-enzymatic biomarkers

- **Determination of Malondialdehyde (MDA) Levels**

Malondialdehyde (MDA) is one of the end products formed during the decomposition of polyunsaturated fatty acids (PUFAs) mediated by free radicals.

MDA levels were determined according to the method of **(Flohé & Günzler, 1984)** This method is based on the colorimetric measurement of the reaction between Thiobarbituric acid (TBA) and MDA in an acidic, high-temperature medium (100 °C), resulting in a reddish-brown chromogen. The intensity of the color is measured at a wavelength of 530 nm.

- ✓ **Experimental protocol:**

- Homogenates were prepared from 200 mg of organ tissue using TP homogenization buffer (pH 7.4).
- The homogenates were centrifuged at 3,000 rpm for 10 minutes at 4 °C.
- A volume of 375 µL of the supernatant was collected.
- To this, 150 µL of TBS buffer solution (50 mM Tris, 150 mM NaCl, pH 7.4) was added.
- Then, 375 µL of TCA-BHT solution (20% trichloroacetic acid, 1% butylated hydroxytoluene) was added to the mixture.
- The mixture was thoroughly mixed and centrifuged at 1,000 rpm for 10 minutes at 4 °C.
- A volume of 400 µL of the resulting supernatant was transferred to a new tube.
- Subsequently, 80 µL of 0.6 M HCl and 320 µL of Tris–TBA solution (26 mM Tris, 120 mM Thiobarbituric acid) were added.
- The mixture was thoroughly mixed and incubated in a water bath at 80 °C for 10 minutes.
- After incubation, the optical density was measured at 530 nm using a spectrophotometer.

The absorbance is directly proportional to the amount of MDA formed, providing an accurate estimation of lipid peroxidation. The concentration of MDA is calculated using the Beer–Lambert law: (DO = E.C.L):

$$[c]\left(\frac{nmol}{mg}ofProtein\right)=\frac{DO\times 10^{6}}{\varepsilon\times L\times X\times Fd}$$

- **c:** Concentration of MDA (nmol/mg of protein).
- **DO:** Optical density measured at 530 nm
- **ε :** Molar extinction coefficient of MDA = 1.56×10^5 $M^{-1}\cdot cm^{-1}$
- **L:** Path length of the cuvette = 1 cm
- **X:** Protein concentration of the sample (mg/mL)
- **Fd:** Dilution factor (Fd = 0.2083).

➢ **Glutathione (GSH) dosage**

The principle of this assay was based on measuring the optical density of 2-nitro-5-mercapturic acid, which resulted from the reduction of 5,5'-dithiobis (2-nitrobenzoic acid) (Ellman's reagent or DTNB) by the sulfhydryl (-SH) groups of glutathione. To protect these -SH groups, the prepared homogenate underwent deproteinization with 0.25% sulfosalicylic acid. This method was originally described by **(Weckbecker & Cory, 1988)**.

✓ **Experimental protocol:**

- Homogenates were prepared from 1 mL of culture using EDTA-phosphate buffer (0.02 M).
- A volume of 0.8 mL of the homogenate was mixed with 0.2 mL of a 0.25% sulfosalicylic acid (SSA) solution.
- The mixture was stirred and incubated for 15 minutes in an ice bath.
- The samples were then centrifuged at 1000 rpm for 5 minutes.
- A volume of 0.5 mL of the resulting supernatant was transferred to a clean tube.
- To this supernatant, 1 mL of Tris-EDTA buffer (0.02 M EDTA, pH 9.6), 0.025 mL of DTNB, and the remaining 0.5 mL of the supernatant were added.

- The mixture was left to stand for 5 minutes at room temperature to allow for

color stabilization; the colorimetric reaction developed instantly.

- Absorbance was measured at 412 nm against a reagent blank.

The concentration of reduced glutathione (GSH) was calculated using the following formula:

$$GSH\left[M\frac{GSH}{mg}GSH/mgdes\ protiènes\right]\frac{DO\times 1\times 1{,}525}{13100\times 0{,}8\times 0{,}5}$$

- **DO:** Optical density measured at 412 nm.
- **1:** Total volume used during deproteinization (0.8 mL of homogenate + 0.2 mL of 0.25% sulfosalicylic acid).
- **1.525:** Total volume used in the GSH determination reaction (0.5 mL of supernatant + 1 mL Tris-EDTA buffer + 0.025 mL DTNB).
- **13100:** Molar extinction coefficient for thiol groups (-SH) at 412 nm (in $M^{-1}\cdot cm^{-1}$).
- **0.8:** Volume (in mL) of the homogenate used.
- **0.5:** Volume (in mL) of the supernatant taken for the assay.

The result expresses the GSH concentration in µmol per mg of protein, which requires that total protein content be quantified in parallel.

1.3.2.2. Enzyme biomarkers:

- **Glutathione peroxidase (GPx) activity assay:**

The enzymatic activity of glutathione peroxidase (GPx) was measured using the method described by **(Flohé & Günzler, 1984)**. This assay is based on the reduction of hydrogen peroxide (H_2O_2) in the presence of reduced glutathione (GSH). During the reaction, GSH is oxidized to glutathione disulfide (H_2O_2) under the catalytic action of GPx, according to the following reaction:

$$H_2O_2 + GSH \xrightarrow{GPx} GSSG + 2H_2O_2$$

This reaction reflects the antioxidant role of GPx in cellular defense against oxidative stress by eliminating peroxides.

✓ **Experimental protocol**

- Homogenates were prepared from 200 mg of tissue using TP homogenization buffer (pH 7.4).
- The homogenates were centrifuged at 3000 rpm for 10 minutes.

- 0.2 mL of the supernatant was collected.
- 0.4 mL of reduced glutathione (GSH, 0.1 mM) was added.
- 0.2 mL of TBS buffer (Tris 50 mM, NaCl 150 mM, pH 7.4) was added.
- The mixture was incubated in a water bath at 25 °C for 5 minutes.
- 0.2 mL of hydrogen peroxide (H_2O_2, 1.3 mM) was added to initiate the reaction, which was allowed to proceed for 10 minutes.
- The reaction was stopped by adding 1 mL of trichloroacetic acid (TCA, 1%).

- The tubes were placed in an ice bath for 30 minutes.
- The samples were centrifuged at 3000 rpm for 10 minutes.
- 0.48 mL of the resulting supernatant was taken.
- 2.2 mL of TBS buffer was added.
- 0.32 mL of CDNB (1 mM) was added.
- The mixture was thoroughly mixed, and the optical density (OD) was measured at 412 nm after 5 minutes.

The enzymatic activity of glutathione peroxidase was calculated using the following formula:

$$GPx(\mu mol.\,mg\ de\ protéine) = \frac{(DOe - DOb).\,0{,}04}{DOb}$$

- OD sample: Optical density of the sample.
- OD standard: Optical density of the standard.
- **0.04**: Final concentration of the GSH substrate in the reaction (in mM).

➢ **Glutathione S-Transferase (GST) activity assay**

Glutathione S-transferase (GST) belongs to a family of primarily cytosolic, multifunctional enzymes involved in intracellular transport, detoxification, and biosynthesis. These enzymes

catalyze conjugation reactions between the endogenous peptide glutathione and various electrophilic compounds.

The activity of glutathione S-transferase is measured using the method described by (**Habig et *al*., 1974)**, which monitors the kinetics of conjugate formation between reduced glutathione and a model substrate, 1-chloro-2,4-dinitrobenzene (CDNB). This reaction leads to the formation of a glutathione substrate conjugate, which can be quantified spectrophotometrically.

✓ **Experimental protocol:**

- Tissue samples were homogenized in 1 mL of phosphate buffer (0.1 M, pH 6.0).
- The homogenate was centrifuged at 14,000 rpm for 30 minutes.
- The resulting supernatant was collected and used as the enzyme source.
- A volume of 200 µL of the supernatant was mixed with 1.2 mL of a reaction mixture containing CDNB (1 mM) and reduced glutathione (GSH, 5 mM).

    - The reaction mixture was prepared by dissolving 20.26 mg of CDNB and 153.65 mg of GSH in 1 mL of ethanol and adjusting the volume to 100 mL with phosphate buffer (0.1 M, pH 6.0).

- Absorbance was recorded at 340 nm for 1 minute, with measurements taken every 15 seconds.
- A blank was prepared using 200 µL of distilled water in place of the supernatant.
- The absorbance was measured at 340 nm after 30 seconds, then at 1-minute intervals for 3 minutes.

The absorbance was measured at 340 nm after 30 seconds, then at 1-minute intervals for 3 minutes.

$$GST(\text{nmol GST/min/mg protéine}) = \frac{(DO\ \text{échant/min} - DO\ \text{blanc/min})}{9{,}6 \times \text{mg de protéine}}$$

- **ΔDO sample - ΔDO blank:** Difference between the average optical density (OD) per minute of the sample and the blank.

- **ε:** Molar extinction coefficient of CDNB = 9.6 $mM^{-1} \cdot cm^{-1}$
- **L:** Optical path length = 1cm

➢ **Catalase activity assay (CAT)**

The spectrophotometric determination of catalase (CAT) activity was performed according to the method described by **(Cakmak & Horst, 1991)**. The decrease in absorbance was recorded over a period of three minutes at a wavelength of 240 nm using a spectrophotometer. The extinction coefficient used for the calculation was **ε = 39,400 $\mu M^{-1} \cdot cm^{-1}$**.

- The reaction mixture had a final volume of 3 mL and contained the following:
- 100 µL of crude enzyme extract,
- 2,850 µL of phosphate buffer (50 mM, pH 7.2),
- 50 µL of hydrogen peroxide solution (0.3%).

The spectrophotometer was calibrated using a blank that did not contain the enzyme extract. The reaction was initiated by the addition of hydrogen peroxide.

1.4. Statistical Analysis

All experimental data were expressed as the mean ± standard deviation (SD) from six independent repetitions (n = 6) for each experimental group. Data visualization, including bar charts and histograms, was performed using Python programming language within the Spyder environment, employing libraries such as Matplotlib and Seaborn for clear and effective graphical representation. Statistical analysis was conducted using Python's SciPy and Stats models libraries to assess differences between control and treated groups. Multiple comparisons were performed using Dunnett's test implemented via Python packages to determine statistical significance relative to the control group. Results were interpreted according to the following significance thresholds:

- **$P > 0.05$**: Not statistically significant
- **$0.05 > P \geq 0.01$** (*): Statistically significant
- **$0.01 > P \geq 0.001$** (**): Highly significant
- **$P < 0.001$** (***): Very highly significant

Results

1. Results

1.1. Effect of NiO_2 Nanoparticle Exposure on Growth Parameters in Rats

The evaluation of growth parameters, including body weight gain and relative organ weights, was conducted throughout the 20-day treatment period with NiO_2 nanoparticles. These general physiological indicators were monitored to assess potential systemic effects and to explore their correlation with the onset of renal and mitochondrial dysfunction induced by nanoparticle exposure.

1.1.1. Weight gain

The analysis of rat body weight across experimental groups revealed a dose-dependent impact of NiO_2 nanoparticle (NP) exposure. Although initial weights were comparable, rats treated with 15 mg/kg/day of NiO_2 NPs exhibited a marked reduction in body weight relative to the control group. This reduction was statistically significant ($P < 0.01$), suggesting systemic toxicity at higher doses. In contrast, rats treated with the moderate dose of 5 mg/kg/day maintained a body weight similar to that of the control group, with no significant difference observed ($P > 0.05$). These findings suggest that high-dose NiO_2 NP exposure impairs overall physiological function, potentially through mitochondrial dysfunction and oxidative stress, ultimately affecting growth and weight maintenance.

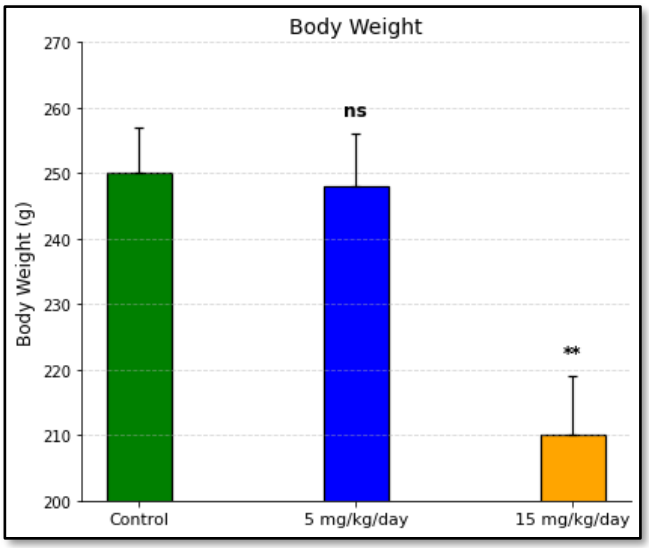


Figure 16: Evolution of the body weight in rats treated for 20 days with NiO_2 NPs.

1.1.2. Relative kidney weight

The analysis of relative kidney weight showed a statistically significant increase ($0.05 > P > 0.01$) in the group exposed to a moderate dose (5 mg/kg/day) of nickel dioxide nanoparticles (NiO_2 NPs) compared to the control group. However, exposure to a higher dose (15

mg/kg/day) resulted in a very highly significant decrease ($P < 0.01$) in relative kidney weight. This biphasic response suggests that while lower doses may induce renal hypertrophy, possibly as a compensatory mechanism, higher doses could lead to structural damage or atrophy, potentially linked to mitochondrial impairment induced by NiO_2 NP toxicity.

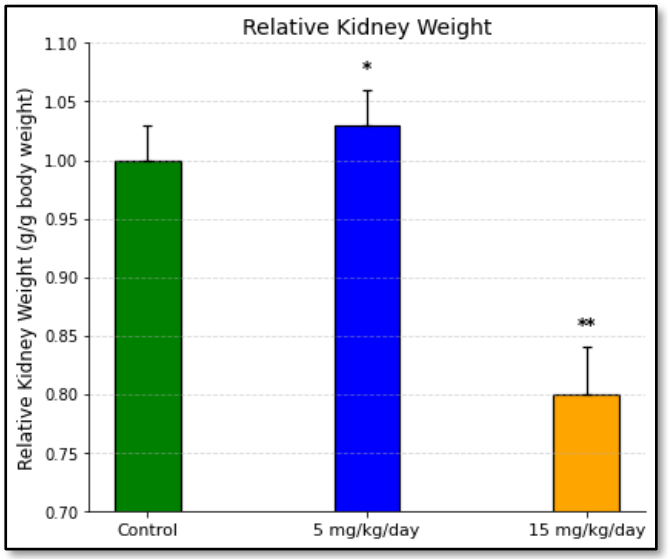


Figure 17: Evolution of the relative weight of the brain in rats treated for 20 days with NiO_2 NP.

1.2. Effect of Nickel dioxide treatment on kidney metabolites

This section aims to investigate the effect of nickel dioxide (NiO_2) nanoparticles on the biochemical composition of rat kidney tissue. Specifically, it involves the quantification of total protein and lipid levels after a 20-day exposure period.

1.2.1. Effect on kidney protein levels

Our findings reveal a significant alteration in kidney protein levels in rats exposed to NiO_2 nanoparticles. Specifically, a marked increase was observed in the group treated with 5 mg/kg compared to the control group, while a notable decrease was seen in the group treated with the higher dose of 15 mg/kg. The differences between the treated groups are statistically significant, indicating a dose-dependent response. These variations in protein concentration are illustrated in Figure (18).

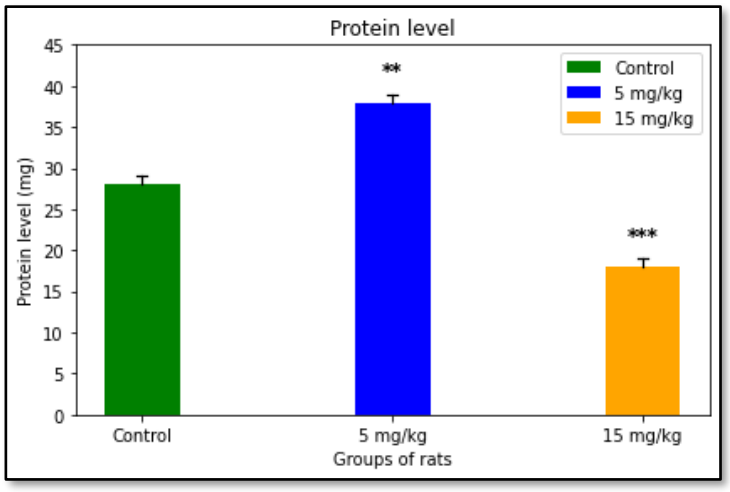


Figure 18: Variation in kidney protein levels of control and treated rats after 20 days of NiO_2 NP exposure.

1.2.2. Effect on the lipid level of the kidney

Our results show a very highly significant decrease ($P < 0.001$) in kidney lipid levels in rats treated with nickel nanoparticles. Both 5 mg/kg and 15 mg/kg doses led to reduced lipid amounts compared to the control group, with the decrease being more pronounced at 15 mg/kg, indicating a dose-dependent effect. These findings suggest a disruption of lipid metabolism in renal tissue.

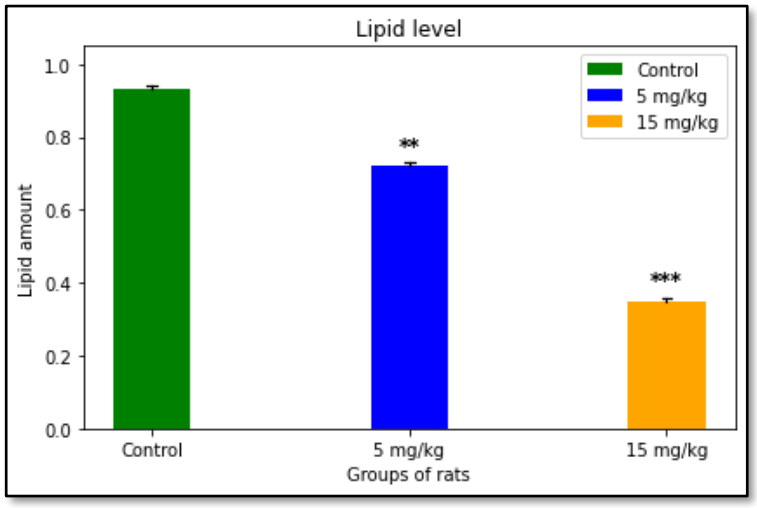


Figure 19: Variation in kidney lipid levels of control and treated rats after 20 days of NiO_2 NP exposure.

1.3. Treatment effect on non-enzymatic parameters

1.3.1. Treatment effect on the level of Malondialdehydes on kidneys

The results show a significant increase ($0.01 > P > 0.001$) in kidney MDA levels in rats treated with 5 mg/kg of NiO_2 nanoparticles and a highly significant increase ($P < 0.001$) at 15 mg/kg compared to the control. This dose-dependent rise in MDA indicates increased oxidative stress and lipid peroxidation in kidney tissue following NiO_2NP exposure.

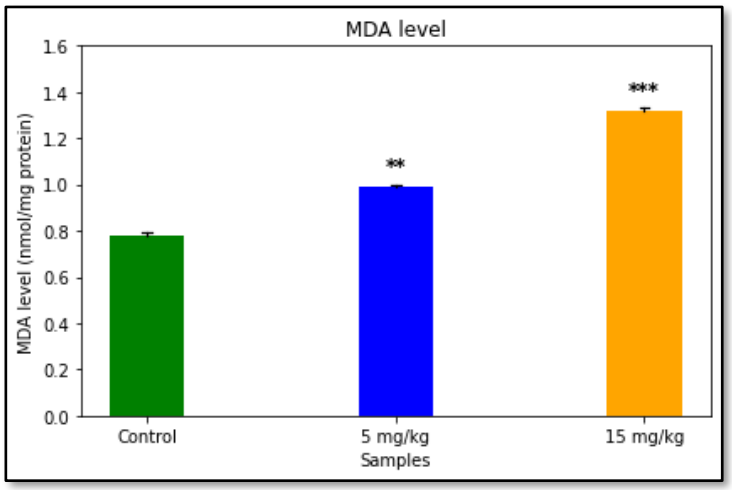


Figure 20: Variation in MDA levels in the kidneys of control and treated rats after 20 days of treatment.

1.3.2. Effect of treatment on the level of GSH

The GSH level in the control group was the highest (1.263 µmol/g tissue), while a notable decrease was observed at 5 mg/kg (0.834 µmol/g tissue). At 15 mg/kg, GSH levels rose to
1.045 µmol/g but remained lower than the control. Error bars (±SD) indicate minimal variability across groups, suggesting that the results are consistent.

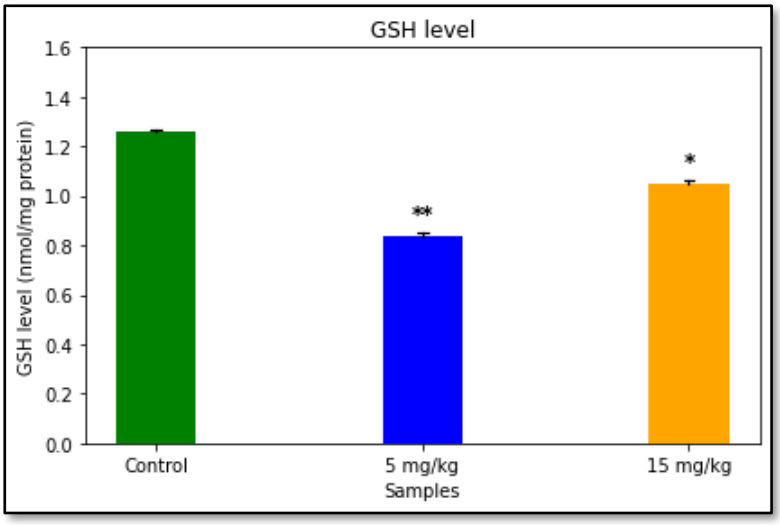


Figure 21: Variation in GSH levels in the kidneys of control and treated rats after 20 days of treatment.

1.4. Effect of NiO_2 nanoparticle exposure on enzymatic parameters in the kidneys of rats

1.4.1. Effect of NiO_2 nanoparticle exposure on glutathione S-transferase activity in rat kidneys

NiO_2 nanoparticle exposure caused a dose-dependent alteration in GST activity. A significant increase at 5 mg/kg ($p < 0.05$) suggests an adaptive antioxidant response. In contrast, a significant decrease at 15 mg/kg ($p < 0.05$) indicates enzyme inhibition and oxidative stress. These results suggest that low doses may enhance defense mechanisms, while higher doses impair them.

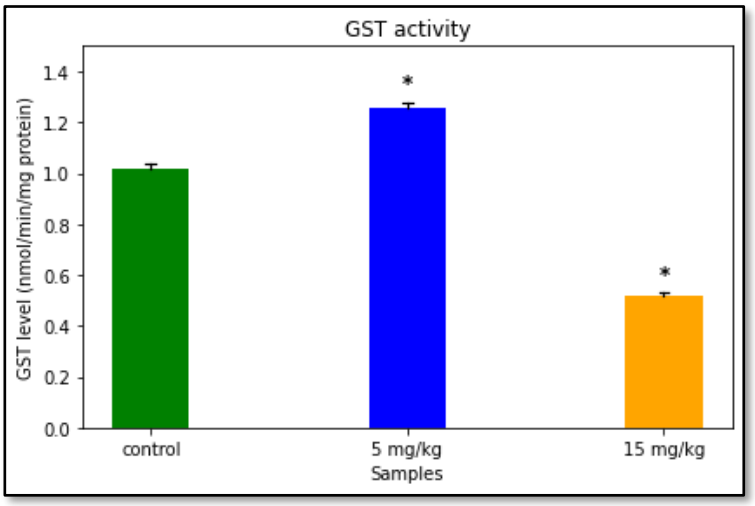


Figure 22: Variation in kidney GST activity in control and NiO_2 NP-treated rats after 20 days of exposure.

1.4.2. Effect of NiO_2 nanoparticle exposure on catalase activity in the kidneys of rats

Catalase activity in rat kidneys was significantly affected by nickel dioxide nanoparticle exposure. At 5 mg/kg, catalase activity increased significantly compared to the control ($p < 0.05$), suggesting an adaptive antioxidant response. However, at 15 mg/kg, catalase activity decreased highly significantly ($p < 0.01$) relative to both the control and 5 mg/kg groups, indicating enzyme inhibition and oxidative stress at higher nanoparticle doses.

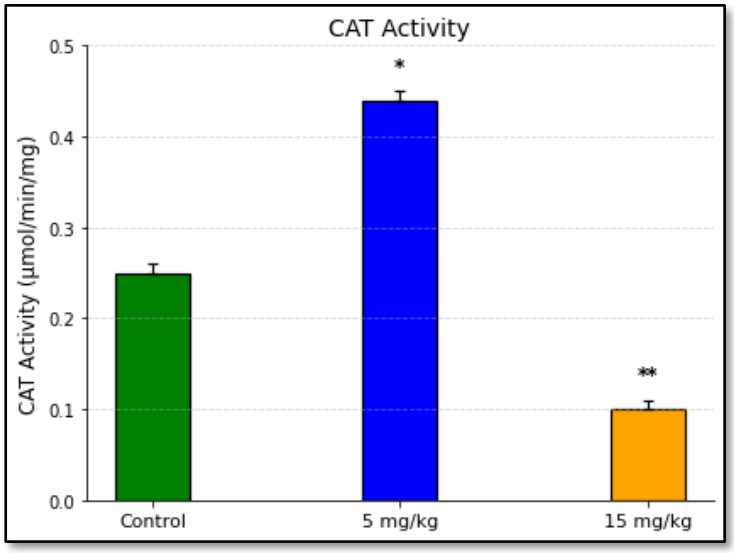


Figure 23: Variation in catalase (CAT) activity in the kidneys of control and NiO_2 NP-treated rats after 20 days of exposure.

1.4.3. Effect of NiO_2 nanoparticle treatment on glutathione peroxidase activity in the kidneys of rats

GPx activity in the control group was 0.456 ± 0.009 U/mg protein. A significant increase was observed at 5 mg/kg (0.734 ± 0.007, $p < 0.01$), while a significant decrease occurred at 15 mg/kg (0.348 ± 0.008, $p < 0.001$). This suggests a biphasic response, with antioxidant activity enhanced at a lower dose and suppressed at a higher one.

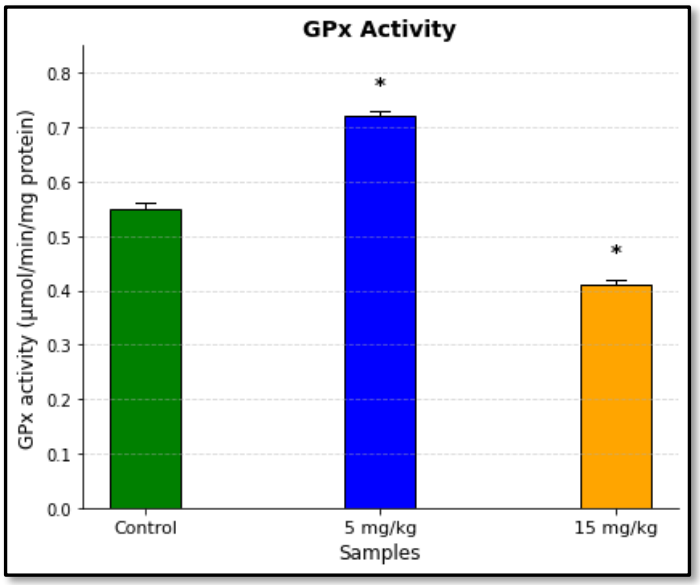


Figure 24: Variation in glutathione peroxidase (GPx) activity in the kidneys of control and NiO_2 NP-treated rats after 20 days of exposure.

1.5. Effect on mitochondria

1.5.1. Mitochondrial swelling

A clear dose-dependent increase in mitochondrial swelling was observed following exposure to NiO_2 nanoparticles. The control group exhibited the lowest optical density value (0.839), indicating minimal mitochondrial swelling under physiological conditions. In contrast, administration of 5 mg/kg NiO_2 nanoparticles resulted in a moderate increase in optical density (0.994), marking the onset of mitochondrial structural alteration. The highest dose group (15 mg/kg) displayed a pronounced elevation in optical density (1.548), reflecting substantial mitochondrial swelling.

These results underscore the detrimental effect of NiO_2 nanoparticles on renal mitochondrial integrity, as demonstrated by the progressive increase in swelling with higher nanoparticle concentrations. The data support the hypothesis that NiO_2 nanoparticles compromise mitochondrial membrane stability, potentially leading to increased permeability and disruption of mitochondrial function.

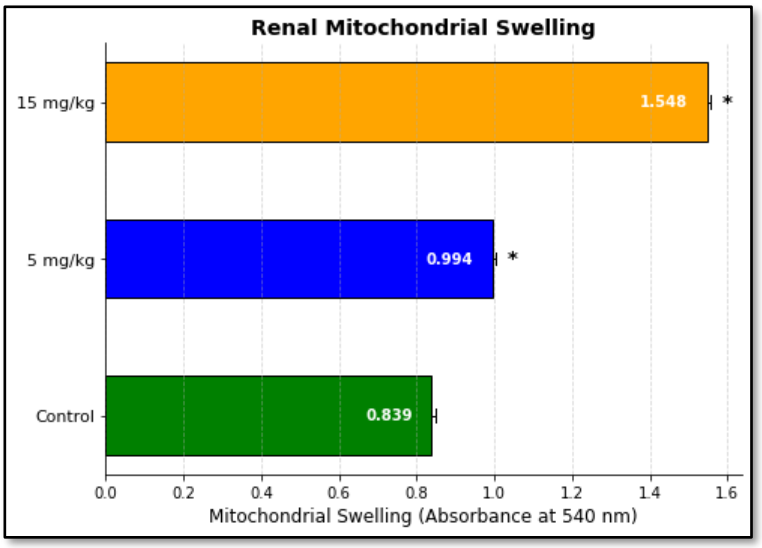


Figure 25: Variation in renal mitochondrial swelling of control and NiO_2 nanoparticle-treated rats after 20 days of treatment.

1.5.2. Mitochondrial Respiration

Mitochondrial respiration exhibited a progressive increase over time across all groups. However, the control group demonstrated a significantly higher rate of oxygen consumption compared to both NiO_2 treated groups. The 15 mg/kg dose induced a marked and sustained reduction in respiratory activity at all measured time points, with statistically significant differences observed versus the control group ($p < 0.01$) and the 5 mg/kg group ($p < 0.05$). These findings confirm a dose-dependent inhibitory effect of NiO_2 nanoparticles on mitochondrial respiratory function.

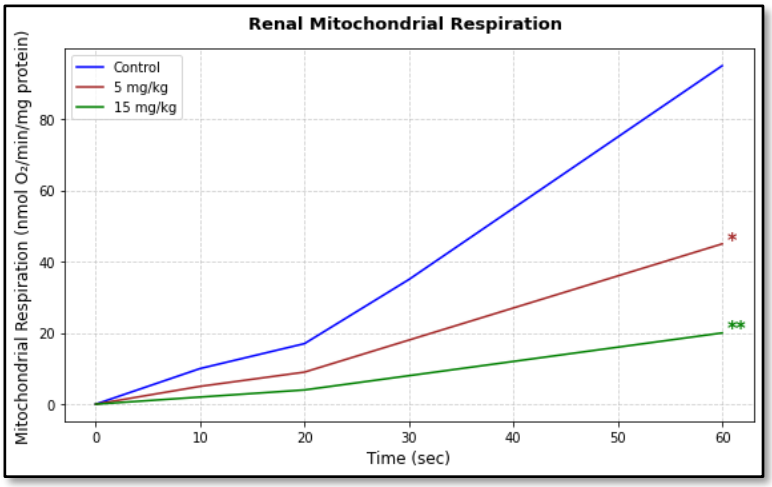


Figure 26: variation in renal mitochondrial respiration of control and NiO_2 nanoparticle treated rats after 20 days of treatment.

Discussion

1. Discussion

Nickel dioxide nanoparticles (NiO_2-NPs) have been widely used in industrial and medical applications. However, concerns remain regarding the safety of exposure to NiO_2-NPs, particularly at varying doses.

In this study, we investigated the potential renal toxicity of NiO_2-NPs using Wistar rats as an anatomical model, administering two different concentrations. First, we explain the rationale for selecting different NiO_2-NP concentrations based on the toxicological principle of the dose- response relationship.

Finally, we discuss the effects of nickel nanoparticles on overall growth (body weight and relative kidney weight), as well as their impact on bimolecular levels (proteins, lipids) and markers of oxidative stress (MDA, GPx, CAT, GSH, and GST).

1.1. Effect on body weight

The observed reduction in body weight at the higher dose of NiO_2 nanoparticles points to a clear physiological toll on the animals. This kind of weight loss doesn't just reflect nutritional issues, it often signals deeper biological disruptions. When the body is under stress, especially from something as disruptive as nanoparticles, energy resources may be diverted toward coping mechanisms, including detoxification and inflammation, rather than growth and maintenance. At 15 mg/kg/day, the body seems to struggle to keep up, which could explain the noticeable drop in weight.

This finding is consistent with the study by **(Luaibi & Zayed, 2018)**, who also reported a significant decrease in body weight in rats exposed to high doses of ZnO nanoparticles, supporting the idea that nanoparticle-induced stress can impair normal physiological growth. Similarly, **(Song et *al*., 2009)** found that zinc-related treatment led to reduced weight gain in rats, further supporting the link between zinc exposure and impaired weight regulation.

On the other hand, the stability of body weight in the group treated with 5 mg/kg/day suggests that the rats may still be within a threshold where compensatory mechanisms are effective. The absence of significant weight change doesn't necessarily mean the nanoparticles had no impact, but rather, that the organism may still be managing the stress without obvious outward signs like

weight loss. A related observation was reported by **(Yu et *al*., 2018)**, who found that low-

dose exposure to nano-NiO (0.24 mg/kg) significantly increased liver wet weight and liver-to-body weight ratio in rats, indicating early physiological adaptations or tissue responses to nanoparticle exposure. This contrast between the two doses highlights how even small differences in exposure can lead to very different biological outcomes.

1.2. Effect on Kidney Weight

The changes in kidney weight offer additional insight into how the body responds to NiO_2 nanoparticles at different exposure levels. The increase in relative kidney weight at the moderate dose may reflect an adaptive enlargement of the organ potentially a response to early cellular stress or mild damage. When the kidney is faced with a toxic challenge, it can sometimes swell or increase in size as part of a compensatory effort to maintain filtration and homeostasis. This observation is in line with the findings of **(Luaibi & Zayed, 2018)**, who similarly reported an increase in kidney weight following exposure to metal-based nanoparticles, suggesting a shared physiological response linked to early nephrotoxic stress.

However, the sharp drop in kidney weight seen at the higher dose tells a more concerning story. Rather than adapting, the tissue may be breaking down, shrinking due to damage, inflammation, or even loss of functional cells. This drop likely reflects structural impairment, signaling that the kidney can no longer keep up with the damage being done. While the increase at low doses might indicate a warning phase, the decrease at high doses suggests that the organ is moving into a state of dysfunction. A similar pattern was reported by **(Dumala et *al*., 2019)**, who observed a decrease in liver weight following exposure to nickel oxide. Although their study focused on a different compound and organ, the downward trend aligns with our findings, highlighting the systemic toxicity potential of nickel-based nanoparticles.

1.3. Effects on the rate of metabolites

1.3.1. Effects on protein levels

The patterns we observed in this study reflect what has been described in earlier research on metal-based nanoparticles. Specifically, the way kidney protein levels increased with a low dose of nickel dioxide and dropped at a higher dose resembles a biphasic or dose-dependent

response. This kind of effect where low exposure might support cellular activity while

high exposure becomes harmful is well-known in toxicology.

One explanation for the protein increase at 5 mg/kg/day may be the activation of mild cellular stress responses. As **(Nikolova & Chavali, 2020)** noted, low concentrations of metal oxide nanoparticles can sometimes enhance certain protective mechanisms in cells, stimulating protein expression or stress-related pathways. At the same time, when the exposure increases, those same particles can disrupt normal cellular functions, leading to damage or loss of proteins.

Our findings at the higher dose (15 mg/kg/day) are consistent with studies showing that metal nanoparticles, including nickel oxide, can generate oxidative stress and impair kidney function. For instance, **(Ahamed et *al.*, 2013)** found that nickel oxide nanoparticles caused oxidative DNA damage and reduced viability in human cells, especially at higher concentrations. This suggests that excessive exposure might impair protein synthesis or lead to degradation of proteins due to cellular injury.

Altogether, our results add to the growing evidence that nanoparticles do not follow a straightforward "more is worse" or "less is safe" model. Instead, biological responses vary with dose, exposure time, and nanoparticle properties. This highlights the need for precise dose control, especially when working with substances like nickel dioxide that may have both beneficial and harmful effects depending on the level of exposure.

1.3.2. Effects on lipid levels

In this study, we observed that exposure to nickel dioxide nanoparticles (NiO NPs) led to a clear, dose-dependent decrease in lipid levels in the kidneys of rats. This suggests that NiO NPs interfere with normal lipid metabolism in kidney tissue, which could contribute to nephrotoxicity.

These findings are consistent with previous research highlighting oxidative stress as a key mechanism by which NiO NPs cause damage. For instance, **(Ahamed et *al.*, 2013)** demonstrated that NiO nanoparticles induce oxidative damage and disrupt cellular functions in multiple organs, including the kidneys.

Our observation that higher doses produced more pronounced lipid reduction aligns with **(Dumala et *al.*, 2019)**, who showed that increasing NiO NP concentrations intensify oxidative stress and worsen kidney function in animal models . This supports the idea of a

dose-dependent toxic effect.

Toxicity of NiO_2 nanoparticles may vary based on size and surface properties, affecting their interaction with kidney cells. Overall, the findings show that NiO nanoparticles can disrupt lipid metabolism and harm kidney function, emphasizing the need for controlled exposure.

3.3. Effects on the rate of biomarkers of oxidative stress

3.3.1. Effect of Nio2 nanoparticle on glutathione (GSH)

Glutathione (GSH) serves as a central component of the cellular antioxidant defense system, safeguarding cells against reactive oxygen species (ROS) and maintaining redox homeostasis. The significant decrease in GSH levels following 5 mg/kg treatment implies enhanced oxidative stress or direct GSH consumption due to increased ROS generation. This observation is consistent with prior findings showing GSH depletion as a sensitive indicator of oxidative burden in tissues **(Sies, 1999) (Zhang et *al.*, 2021) .**

Supporting our results**, (Sahu et *al.*, 2013)** also showed a dose-dependent decrease in intracellular GSH levels after 24 h exposure to ZnO NPs.

Interestingly, the partial restoration of GSH levels at 15 mg/kg may reflect an adaptive cellular response, potentially mediated by transcriptional upregulation of GSH-synthesizing enzymes or activation of the Nrf2 pathway a critical regulator of antioxidant defense **(Kensler et *al.*, 2007)**. Although not returning to baseline levels, the increase suggests a dose-dependent compensation mechanism may be at play.

This biphasic pattern is often associated with hormesis, where low doses trigger stress, while higher doses initiate protective pathways. Such findings warrant careful dose optimization in therapeutic contexts to avoid detrimental redox imbalances.

3.3.2. Effect of Nio2 nanoparticle on glutathione peroxidase (GPX)

Glutathione peroxidase (GPx) plays a vital role in protecting cells by breaking down harmful hydrogen peroxide and lipid peroxides, which can otherwise cause oxidative damage. In

this study, the increase in GPx activity observed at the 5 mg/kg dose likely represents the body's attempt to boost its antioxidant defenses in response to increased oxidative stress.

This kind of adaptive response is well-supported by previous research **(Brigelius-Flohé&Maiorino, 2013).**

On the other hand, the marked decrease in GPx activity at the higher 15 mg/kg dose suggests that excessive exposure might overwhelm the cell's protective mechanisms. When oxidative stress becomes too intense, it can actually impair or reduce the activity of important enzymes like GPx **(Arthur, 2001)**. This kind of biphasic, or "two-phase," response where low doses trigger a protective effect but higher doses cause harm is a pattern commonly seen in studies of oxidative stress.

Overall, these results highlight the need to carefully balance dosing in treatments aimed at modulating oxidative stress, to maximize benefits without causing unintended damage.

3.3.3. Effect of Nio2 nanoparticle on catalase.

Our results revealed that catalase activity in rat kidneys was significantly influenced by nickel dioxide nanoparticles (NiO NPs) in a dose-dependent manner. At the lower dose (5 mg/kg), catalase activity increased significantly, which may reflect a protective, adaptive response to oxidative stress. However, at the higher dose (15 mg/kg), catalase activity decreased markedly, suggesting enzyme inhibition and impaired antioxidant defense as observed in the study of **(Hussain et *al*., 2020)**.

This pattern is consistent with earlier studies showing that low-level nanoparticle exposure can stimulate antioxidant enzymes as part of a defensive mechanism, while higher exposures overwhelm these defenses, leading to oxidative damage **(Ahamed et *al*., 2013) (Dumala et *al*., 2019)**. **(Hashim et *al*., 2022)** reported increased catalase (CAT) activity in kidneys exposed to metal oxide nanoparticles, associating this rise with nephrotoxicity."

The dose-dependent modulation of catalase underscores the complex biological responses to NiO nanoparticles and highlights the risk of kidney injury associated with higher nanoparticle concentrations.

3.3.4. Effect on the level of Malondialdehydes,

This study found that rats exposed to nickel dioxide nanoparticles (NiO_2NPs) had significantly higher levels of malondialdehyde (MDA) in their kidney tissues, especially at higher doses. Since MDA is a key indicator of oxidative stress and lipid damage, this

suggests that the NiO_2NPs triggered harmful oxidative processes in the kidneys.

These results are in agreement with previous research. For instance, **(Hussain et *al.*, 2020)** observed similar increases in MDA levels after exposure to nickel oxide nanoparticles, pointing to oxidative stress as a main contributor to kidney damage.

Similarly, **(Siddiqui et *al.*, 2012)** reported a significant, dose-dependent increase in MDA levels in HEp-2 and MCF-7 cells exposed to NiO nanoparticles. Although their study was conducted in vitro and on a different organ system, their findings support our results by confirming that nickel-based nanoparticles can induce lipid peroxidation and elevate MDA levels, reflecting oxidative damage.

(Delavar et *al.*, 2025) also reported a significant rise in MDA levels following exposure to NiO nanoparticles, and showed that co-treatment with curcumin nanoparticles could reduce this oxidative effect, especially when exposure time was shortened. Their findings further confirm that NiO-based nanoparticles promote oxidative stress through lipid peroxidation.

The stronger effect we saw at the 15 mg/kg dose suggests that higher amounts of NiO_2NPs cause more damage. This could happen because the nanoparticles build up in the kidney and disturb how mitochondria work. When mitochondria are affected, they can produce too many reactive oxygen species (ROS), which harm parts of the cell like lipids, proteins, and DNA. The increase in MDA levels in our results clearly shows that these nanoparticles lead to oxidative stress and damage in kidney tissues.

3.3.5. Effect of NiO_2 nanoparticle exposure on GST

In this study, exposure to NiO_2 nanoparticles caused significant changes in GST activity in the kidneys, depending on the dose. At 5 mg/kg, there was a noticeable increase in GST activity, which likely reflects the body's attempt to defend itself against mild oxidative stress by boosting

its detoxification enzymes. However, at 15 mg/kg, GST activity dropped significantly, suggesting that at higher doses, the antioxidant system becomes overwhelmed or that the enzyme itself may be inhibited.

A similar pattern was seen in the study by **(Amani et *al*., 2022)**, where GST activity went up at lower concentrations of silver nanocolloids. Just like in our research with NiO_2 nanoparticles, this increase likely shows the cells trying to protect themselves from stress. However, in both cases, GST levels changed depending on how much of the nanoparticles were given and for how long, which suggests that with stronger or longer exposure, the body's defense system may start to break down or become less effective.

Likewise, **(Delavar et *al*., 2025)** found that exposure to NiO nanoparticles significantly increased GST activity, and that co-treatment with curcumin nanoparticles helped reduce this increase, especially when exposure duration was shorter. This supports the idea that while GST initially rises in response to oxidative stress, prolonged or high-dose exposure may require antioxidant support to prevent damage or enzyme exhaustion.

(Bergmann & Graça, 2020) further supports this, showing GST activity decrease after prolonged exposure, even without dose variation, highlighting how duration alone can impair antioxidant defense.

Reduced GST activity at high nanoparticle doses may worsen kidney damage by weakening detoxification and oxidative balance, while low doses may trigger a temporary protective response.

1.4. Effect on Mitochondrial swelling

Our results show a clear trend: the higher the dose of NiO_2 nanoparticles, the greater the swelling of renal mitochondria. In the control group, where no nanoparticles were introduced, mitochondria maintained their normal structure, as expected under healthy conditions. However, when exposed to a low dose (5 mg/kg), we began to see signs of stress, a noticeable increase in swelling that suggests the mitochondrial membranes were starting to lose their stability. This effect became much more pronounced at the higher dose (15 mg/kg), where the extent of swelling pointed to significant structural damage. This pattern strongly suggests that NiO_2 nanoparticles disrupt mitochondrial function in a dose-dependent manner. As the exposure increases, the membrane

likely becomes more permeable, allowing fluids and ions to pass through more freely, which leads to swelling **(AshaRani et *al*., 2009)**.

This disruption not only affects mitochondrial structure but may also compromise

their ability to produce energy efficiently **(Li et *al.*, 2016),** ultimately putting kidney cell health at risk. Similar observations have been made by **(Germande et *al.*, 2022)**, who reported a concentration- dependent loss of mitochondrial membrane potential (ΨM P) upon NiONP exposure, indicating a corresponding disruption in mitochondrial function, which could lead to swelling and impaired respiration.

(Faisal et *al.*, 2016) showed that cobalt oxide nanoparticles (Co_3O_4-NPs) caused mitochondrial swelling, DNA damage, and apoptosis in eggplant cells, primarily through oxidative stress and nitric oxide signaling. The study highlights mitochondrial dysfunction as a key mechanism of nanoparticle toxicity.

(Pereira et *al.*, 2018) demonstrated that iron oxide nanoparticles (Fe_3O_4-NPs) induce mitochondrial damage in rats, evidenced by oxidative stress, enzyme imbalance, and increased cytochrome c. Co-treatment with diferuloylmethane (DFM) significantly reduced these effects, highlighting its protective antioxidant and anti-apoptotic potential against Fe_3O_4-NP-induced mitochondrial toxicity.

(Zhuo et *al.*, 2024) showed that zinc oxide nanoparticles (ZnO-NPs) induce mitochondrial damage in lung cells, marked by loss of mitochondrial membrane potential and increased ROS production. This mitochondrial dysfunction triggered NLRP3 inflammasome activation, leading to inflammation and acute lung injury. The findings highlight mitochondrial injury as a key mechanism in ZnO-NP-induced pulmonary toxicity.

Conversely**, (Mallick et *al.*, 2016)** designed mitochondria-targeted nanoparticles carrying pro- apoptotic agents that effectively accumulated in cancer cell mitochondria. These nanoparticles induced mitochondrial outer membrane permeabilization, cytochrome c release, and caspase activation, leading to apoptosis. The study highlights the potential of mitochondria-targeted nanocarriers for enhancing cancer therapy through mitochondrial disruption.

Furthermore, Fe_3O_4 nanoparticles, though widely used in biomedical applications, have been shown to induce neurotoxicity through mitochondrial dysfunction. In a study on rabbits, exposure to Fe_3O_4-NPs (200–300 μg/kg) increased lipid peroxidation, protein oxidation, and ROS levels in the brain. This was accompanied by elevated mitochondrial enzyme activity and swelling, reduced mitochondrial respiration, and increased caspase-3

and TNF-α levels, indicating oxidative stress, inflammation, and apoptosis. These findings highlight the role of Fe_3O_4-NP-induced mitochondrial damage in promoting neurotoxic and potentially neurodegenerative effects **(Chahinez et *al.*, 2016)**.

Similarly, **(Guo et *al.*, 2018)** found that silica nanoparticles (SiNPs) damage mitochondria in endothelial cells. They increased oxidative stress, reduced the energy production (ATP), and disrupted the mitochondrial membrane. SiNPs also caused the mitochondria to break apart more often (fission) and blocked their natural renewal process by lowering key regulatory proteins like PGC-1α, NRF1, and TFAM. This mitochondrial damage was a major cause of cell injury.

In the same way**, (Ghanbary et *al.*, 2018)** showed that titanium dioxide nanoparticles (TiO_2- NPs) can harm human monocytes. After 12 hours of exposure to 10 μg/ml, the cells showed signs of stress and damage, including more reactive oxygen species (ROS), loss of mitochondrial membrane potential, damage to lysosomes, increased fat oxidation, and lower levels of glutathione. These findings suggest that TiO_2-NPs cause oxidative stress and organelle damage, and that using antioxidants might help reduce their harmful effects.

1.5. Effect on Mitochondrial Respiration

The mitochondrial respiration results revealed a concerning pattern. Although oxygen consumption increased over time in all groups as expected under normal mitochondrial function, the control group clearly exhibited superior performance. Their mitochondria maintained efficient and steadily rising respiratory activity. In contrast, exposure to NiO_2 nanoparticles, particularly at the higher 15 mg/kg dose, led to a marked reduction in this activity.

The mitochondria appeared to be functioning under stress, with significantly lower oxygen consumption indicating impaired energy production **(Smith et *al.*,2020)**. This suggests that the nanoparticles may be interfering with the mitochondrial respiratory chain possibly through membrane disruption or oxidative stress. The 5 mg/kg dose produced a milder effect, pointing to a

dose-dependent impact. In essence, the greater the exposure to NiO_2, the more mitochondrial function was compromised. Given the central role of mitochondria in cellular

energy balance, such impairment could have serious implications for kidney health, especially with prolonged or high- level exposure **(Zhao et *al.*, 2015)**.

In line with this, **(Freyre-Fonseca et *al.*, 2011)** demonstrated similar disruptions in mitochondrial respiration caused by titanium dioxide nanoparticles (TiO_2 NPs). Their study showed that TiO_2 NPs reduced NADH levels, disturbed the mitochondrial membrane potential, and impaired respiratory function in lung mitochondria, leading to increased reactive oxygen species production. This further supports the idea that nanoparticle exposure can directly damage the mitochondrial respiratory chain, compromising energy production and increasing oxidative stress.

Similarly, **(Z. Zhang et *al.*, 2024)** examined how silver (AgNPs), silicon dioxide (SiNPs), and gold (AuNPs) nanoparticles affect mitochondria in macrophages at safe doses. They found that AgNPs and SiNPs—but not AuNPs—caused mitochondrial damage by lowering membrane potential, disrupting structure, increasing ROS, and reducing ATP production. These nanoparticles also impaired mitochondrial respiration by reducing genes involved in complexes I, III, and IV. Smaller particles were more harmful, but the type of nanoparticle was the main factor in mitochondrial toxicity. This study highlights how nanoparticle composition critically influences mitochondrial health.

(Li et *al.*, 2012) studied the toxicity of zinc oxide nanoparticles (ZnO NPs) on isolated rat liver mitochondria. They found that ZnO NPs caused membrane potential loss, swelling, increased permeability, respiratory depression, cytochrome c release, and ROS generation. These effects impair mitochondrial respiration and promote oxidative stress and energy loss, potentially triggering apoptosis. The study offers important insights into how ZnO NPs damage mitochondria.

Conclusion

Conclusion

This study was dedicated to evaluating the effects of of nickel dioxide nanoparticles (NiO_2 NPs) administered in increasing doses on renal metabolic and mitochondrial parameters in Wistar rats. Our objective was to assess the alterations in proteins, lipids, oxidative stress markers both non-enzymatic (GSH, MDA) and enzymatic (GPx, GST, CAT), as well as mitochondrial functionality, namely swelling and respiratory activity.

In light of our experimental results, we can conclude that:

- Oral administration of NiO_2 NPs resulted in a dose-dependent biphasic change in relative kidney weight, with a significant increase at moderate dose (5 mg/kg/day), potentially indicating renal hypertrophy, and a very highly significant decrease at high dose (15 mg/kg/day), suggestive of tissue atrophy likely associated with mitochondrial dysfunction.
- Protein concentrations were found to increase at the moderate dose, indicating a compensatory cellular response, whereas a notable decline was observed at the higher dose, pointing toward structural degradation or inhibited synthesis under toxic conditions.
- Lipid levels showed a decrease across both treatment groups, which may reflect membrane lipid peroxidation or impaired lipid metabolism due to oxidative damage.
- Evaluation of oxidative stress revealed a consistent increase in MDA levels in both exposed groups, reinforcing the occurrence of lipid peroxidation. In parallel, GSH levels were depleted, suggesting a weakening of the non-enzymatic antioxidant defense system.
- Enzymatic antioxidant responses (GPx, GST, CAT) exhibited a stimulatory effect at the moderate dose, followed by a marked inhibition at the higher dose, confirming an adaptive phase followed by toxic collapse of antioxidant capacity under excessive nanoparticle load.
- At the mitochondrial level, mitochondrial swelling increased significantly with dose, indicating membrane permeability transition and dysfunction. Likewise, mitochondrial
- respiration was impaired in a dose-dependent manner, suggesting that NiO_2 NPs compromise oxidative phosphorylation efficiency and thus cellular energy production.
- Altogether, our findings highlight that nickel dioxide nanoparticles induce dose-

dependent renal toxicity through disruption of metabolic balance and impairment of mitochondrial integrity, potentially mediated by oxidative stress pathways.

References

References

A

- Abd-Eltawab Tammam, A., A. Khalaf, A. A., R. Zaki, A., Mansour Khalifa, M., A. Ibrahim, M., M. Mekkawy, A., E. Abdelrahman, R., Farghali, A., & A. Noshy, P. (2022). Hesperidin protects rats' liver and kidney from oxidative damage and physiological disruption induced by nickel oxide nanoparticles. *Frontiers in Physiology*, *13*. https://doi.org/10.3389/fphys.2022.912625

- Abudayyak, M., Guzel, E., & Özhan, G. (2017). Nickel Oxide Nanoparticles Induce Oxidative DNA Damage and Apoptosis in Kidney Cell Line (NRK-52E). *Biological Trace Element Research*, *178*(1), 98–104. https://doi.org/10.1007/s12011-016-0892-z

- Ahamed, M., Ali, D., Alhadlaq, H. A., & Akhtar, M. J. (2013). Nickel oxide nanoparticles exert cytotoxicity via oxidative stress and induce apoptotic response in human liver cells (HepG2). *Chemosphere*, *93*(10), 2514–2522. https://doi.org/10.1016/j.chemosphere.2013.09.047

- Alhazmi, A. I., El-Refaei ,Mohamed F., & and Abdallah, E. A. A. (2024). Protective effects of gallic acid against nickel-induced kidney injury: Impact of antioxidants and transcription factor on the incidence of nephrotoxicity. *Renal Failure*, *46*(1), 2344656. https://doi.org/10.1080/0886022X.2024.2344656

- Al-Naimi, M. S., Rasheed, H. A., Hussien, N. R., Al-Kuraishy, H. M., & Al-Gareeb, A. I. (2019). Nephrotoxicity: Role and significance of renal biomarkers in the early detection of acute renal injury. *Journal of Advanced Pharmaceutical Technology & Research*, *10*(3), 95–99. https://doi.org/10.4103/japtr.JAPTR_336_18

- Amani, R., Heidari, B., Ghafoori, H., & Valipour, A. (2022). Effects of Silver Nanocolloid and Copper Oxide (I) on HSP70 Expression and GST Activity in the Caspian Kutum. *Turkish Journal of Fisheries and Aquatic Sciences*, *22*(6). https://doi.org/10.4194/TRJFAS19548

- Areecheewakul, S., Adamcakova-Dodd, A., Givens, B. E., Steines, B. R., Wang, Y., Meyerholz, D. K., Parizek, N. J., Altmaier, R., Haque, E., O'Shaughnessy, P. T., Salem, A. K., & Thorne, P. S. (2020). Toxicity assessment of metal oxide nanomaterials using in vitro screening and murine acute inhalation studies. *NanoImpact*, *18*, 100214. https://doi.org/10.1016/j.impact.2020.100214

- Arthur, J. R. (2001). The glutathione peroxidases: *Cellular and Molecular Life Sciences*, *57*(13), 1825–1835. https://doi.org/10.1007/PL00000664

- AshaRani, P. V., Low Kah Mun, G., Hande, M. P., & Valiyaveettil, S. (2009). Cytotoxicity and Genotoxicity of Silver Nanoparticles in Human Cells. *ACS Nano*, *3*(2), 279–290. https://doi.org/10.1021/nn800596w

B

- Barceloux, D. G., & Barceloux, D. (1999). Nickel. *Journal of Toxicology: Clinical Toxicology*, *37*(2), 239–258. https://doi.org/10.1081/CLT-100102423

- Bassaglia, Y. (2004). *Biologie cellulaire* (2e éd). Maloine.

- Bayda, S., Adeel, M., Tuccinardi, T., Cordani, M., & Rizzolio, F. (2020). The History of Nanoscience and Nanotechnology: From Chemical–Physical Applications to Nanomedicine. *Molecules*, *25*(1), Article 1. https://doi.org/10.3390/molecules25010112

- Bergmann, M., & Graça, M. A. S. (2020). Activities of oxidative stress- and cell membrane-related enzymes in a freshwater leaf-shredder exposed to uranium. *Limnetica*, *39*(1), 169–184. https://doi.org/10.23818/limn.39.12

- Bhosale, S. C., Pawara, A. D., Jadhav, B. S., & Hulsinge, R. V. (2024). Nanoparticle classification, physicochemical properties, characterization, and applications: A comprehensive review for biologists. *INTERNATIONAL JOURNAL OF NOVEL RESEARCH AND DEVELOPMENT*, *9*(3), b930–b938.

- Bradford, M. M. (1976). A rapid and sensitive method for the quantitation of microgram quantities of protein utilizing the principle of protein-dye binding. *Analytical Biochemistry*, *72*(1–2), 248–254. https://doi.org/10.1016/0003-2697(76)90527-3

- Brigelius-Flohé, R., & Maiorino, M. (2013). Glutathione peroxidases. *Biochimica et Biophysica Acta (BBA) - General Subjects*, *1830*(5), 3289–3303. https://doi.org/10.1016/j.bbagen.2012.11.020

B.Sc, H. A. (2022, June 1). *What is Nephrotoxicity?* News-Medical. https://www.news-medical.net/life-sciences/What-is-Nephrotoxicity.aspx

Buzea, C., Pacheco, I. I., & Robbie, K. (2007). Nanomaterials and nanoparticles: Sources and

toxicity. *Biointerphases*, *2*(4), MR17–MR71. https://doi.org/10.1116/1.2815690.

C

- Cakmak, I., & Horst, W. J. (1991). Effect of aluminium on lipid peroxidation, superoxide dismutase, catalase, and peroxidase activities in root tips of soybean (Glycine max). *Physiologia Plantarum*, *83*(3), 463–468. https://doi.org/10.1111/j.1399-3054.1991.tb00121.x

- Capasso, L., Camatini, M., & Gualtieri, M. (2014). Nickel oxide nanoparticles induce inflammation and genotoxic effect in lung epithelial cells. *Toxicology Letters*, *226*(1), 28–34. https://doi.org/10.1016/j.toxlet.2014.01.040

- Chahinez, T., Rachid, R., Salim, G., Lamia, B., Ghozala, Z., Nadjiba, T., Aya, S., Sara, H., Hajer, C., Samira, B., Mohamed, K., Mariem, A., & Belgacem, D. (2016). Toxicity of Fe3O4 nanoparticles on oxidative stress status, stromal enzymes and mitochondrial respiration and swelling of Oryctolagus cuniculus brain cortex. *Toxicology and Environmental Health Sciences*, *8*(5), 349–355. https://doi.org/10.1007/s13530-016-0296-7

- Chang, E. S., Song, K., Song, J.-Y., Sung, M., Lee, M.-S., Oh, J. H., Kim, J.-Y., Park, Y. H., Jung, K., & Choi, Y.-L. (2024). Real-time assessment of relative mitochondrial ATP synthesis response against inhibiting and stimulating substrates (MitoRAISE). *Cancer & Metabolism*, *12*(1), 25. https://doi.org/10.1186/s40170-024-00353-3

Cooper, G. M., & François, C. (1999). *La cellule: Une approche moléculaire*. De Boeck université.

D

- Descamps, M.-C. (2008). *Biologie cellulaire: Cours, exercices, annales et QCM corrigés 50 % cours + 50 % exos* (Nouvelle éd.). ÉdiScience.

- Divakaruni, A. S., Paradyse, A., Ferrick, D. A., Murphy, A. N., & Jastroch, M. (2014). Chapter Sixteen—Analysis and Interpretation of Microplate-Based Oxygen Consumption and pH Data. In A. N. Murphy & D. C. Chan (Eds.), *Methods in Enzymology* (Vol. 547, pp. 309– 354). Academic Press. https://doi.org/10.1016/B978-0-12-801415-8.00016-3

- Du, J., Li, Z., Cao, X., Qi, Q., Wang, L., Liu, P., Chen, Y., Hu, G., Guo, X., & Gao, X. (2024). Mechanism of Mitochondrial Kinetic Imbalance and Nrf2 Signaling Pathway-Mediated Oxidative Stress in Nickel and/or Chromium-Induced Kidney Injury in Mice.

Antioxidants, *13*(8), Article 8. https://doi.org/10.3390/antiox13080980

- Dumala, N., Mangalampalli, B., Kalyan Kamal, S. S., & Grover, P. (2019). Repeated oral dose toxicity study of nickel oxide nanoparticles in Wistar rats: A histological and biochemical perspective. *Journal of Applied Toxicology: JAT*, *39*(7), 1012–1029. https://doi.org/10.1002/jat.3790

E

- El-Kemary, M., Nagy, N., & El-Mehasseb, I. (2013). Nickel oxide nanoparticles: Synthesis and spectral studies of interactions with glucose. *Materials Science in Semiconductor Processing*, *16*(6), 1747–1752. https://doi.org/10.1016/j.mssp.2013.05.018

F

- Faisal, M., Saquib, Q., Alatar, A. A., Al-Khedhairy, A. A., Ahmed, M., Ansari, S. M., Alwathnani, H. A., Dwivedi, S., Musarrat, J., & Praveen, S. (2016). Cobalt oxide nanoparticles aggravate DNA damage and cell death in eggplant via mitochondrial swelling and NO signaling pathway. *Biological Research*, *49*(1), 20. https://doi.org/10.1186/s40659- 016-0080-9

- Flohé, L., & Günzler, W. A. (1984). [12] Assays of glutathione peroxidase. In *Methods in Enzymology* (Vol. 105, pp. 114–120). Elsevier. https://doi.org/10.1016/S0076-6879(84)05015-1

- Florance, I., Cordani, M., Pashootan, P., Moosavi, M. A., Zarrabi, A., & Chandrasekaran, N. (2024). The impact of nanomaterials on autophagy across health and disease conditions.

Cellular and Molecular Life Sciences, *81*(1), 184. https://doi.org/10.1007/s00018-024-05199- y

- Forbe, T., García, M., & Gonzalez, E. (2011). Potencial risks of nanoparticles. *Food Science and Technology*, *31*, 835–842. https://doi.org/10.1590/S0101-20612011000400002

- Freyre-Fonseca, V., Delgado-Buenrostro, N. L., Gutiérrez-Cirlos, E. B., Calderón-Torres, C. M., Cabellos-Avelar, T., Sánchez-Pérez, Y., Pinzón, E., Torres, I., Molina-Jijón, E., & Zazueta, C. (2011). Titanium dioxide nanoparticles impair lung mitochondrial function.

Toxicology Letters, *202*(2), 111–119. https://doi.org/10.1016/j.toxlet.2011.01.025

G

- Germande, O., Ducret, T., Quignard, J.-F., Deweirdt, J., Freund-Michel, V., Errera, M.-H., Cardouat, G., Vacher, P., Muller, B., Berger, P., Guibert, C., Baudrimont, M., & Baudrimont, I. (2022). NiONP-Induced Oxidative Stress and Mitochondrial Impairment in an In Vitro

Pulmonary Vascular Cell Model Mimicking Endothelial Dysfunction. *Antioxidants (Basel, Switzerland)*, *11*(5), 847. https://doi.org/10.3390/antiox11050847

- Ghanbary, F., Seydi, E., Naserzadeh, P., & Salimi, A. (2018). Toxicity of nanotitanium dioxide (TiO2-NP) on human monocytes and their mitochondria. *Environmental Science and Pollution Research*, *25*(7), 6739–6750. https://doi.org/10.1007/s11356-017-0974-2

- Ghorbanpour Delavar, M., Ghobadi, S., Vatandoust, S., Manouchehri, H., & Changizi, R. (2025). Protective effect of curcumin-coated chitosan-alginate nanoparticles against oxidative stress induced by nickel oxide nanoparticles in the Gold fish Carassius auratus). *Iranian Journal of Fisheries Sciences*, *24*(2). https://doi.org/10.22092/ijfs.2025.132815

- Gornati, R., Papis, E., Di Gioacchino, M., Sabbioni, E., Dalle-Donne, I., Milzani, A., & Bernardini, G. (2009). *In Vivo* and *In Vitro* Models for Nanotoxicology Testing. In S. C. Sahu & D. A. Casciano (Eds.), *Nanotoxicity* (1st ed., pp. 279–302). Wiley. https://doi.org/10.1002/9780470747803.ch15

- Guo, C., Wang, J., Jing, L., Ma, R., Liu, X., Gao, L., Cao, L., Duan, J., Zhou, X., Li, Y., & Sun, Z. (2018). Mitochondrial dysfunction, perturbations of mitochondrial dynamics and biogenesis involved in endothelial injury induced by silica nanoparticles. *Environmental Pollution*, *236*, 926–936. https://doi.org/10.1016/j.envpol.2017.10.060

H

- Habashi, F. (2013). Nickel, Physical and Chemical Properties. In R. H. Kretsinger, V. N. Uversky, & E. A. Permyakov (Eds.), *Encyclopedia of Metalloproteins* (pp. 1520–1520). Springer. https://doi.org/10.1007/978-1-4614-1533-6_338
- Habig, W. H., Pabst, M. J., & Jakoby, W. B. (1974). Glutathione S-Transferases. *Journal of Biological Chemistry*, *249*(22), 7130–7139. https://doi.org/10.1016/S0021-9258(19)42083-8
- Haleem, A., Javaid, M., Singh, R. P., Rab, S., & Suman, R. (2023). Applications of nanotechnology in medical field: A brief review. *Global Health Journal*, *7*(2), 70–77. https://doi.org/10.1016/j.glohj.2023.02.008
- Hashim, M., Mujahid, H., Hassan, S., Bukhari, S., Anjum, I., Hano, C., Abbasi, B. H., & Anjum, S. (2022). Implication of Nanoparticles to Combat Chronic Liver and Kidney Diseases: Progress and Perspectives. *Biomolecules*, *12*(10), 1337. https://doi.org/10.3390/biom12101337

- Ho, H.-J., & Shirakawa, H. (2023). Oxidative Stress and Mitochondrial Dysfunction in Chronic Kidney Disease. *Cells*, *12*(1), Article 1. https://doi.org/10.3390/cells12010088

- Hussain, M. F., Naeem Ashiq, M., Gulsher, M., Akbar, A., & Iqbal, F. (2020). Exposure to variable doses of nickel oxide nanoparticles disturbs serum biochemical parameters and oxidative stress biomarkers from vital organs of albino mice in a sex-specific manner.

Biomarkers: Biochemical Indicators of Exposure, Response, and Susceptibility to Chemicals, *25*(8), 719–724. https://doi.org/10.1080/1354750X.2020.1841829

J

- Jeevanandam, J., Barhoum, A., Chan, Y. S., Dufresne, A., & Danquah, M. K. (2018). Review on nanoparticles and nanostructured materials: History, sources, toxicity and regulations.

Beilstein Journal of Nanotechnology, *9*(1), 1050–1074. https://doi.org/10.3762/bjnano.9.98

- Joudeh, N., & Linke, D. (2022). Nanoparticle classification, physicochemical properties, characterization, and applications: A comprehensive review for biologists. *Journal of Nanobiotechnology*, *20*(1), 262. https://doi.org/10.1186/s12951-022-01477-8

K

- Kensler, T. W., Wakabayashi, N., & Biswal, S. (2007). Cell Survival Responses to Environmental Stresses Via the Keap1-Nrf2-ARE Pathway. *Annual Review of Pharmacology and Toxicology*, *47*(1), 89–116. https://doi.org/10.1146/annurev.pharmtox.46.120604.141046

- Khan, I., Saeed, K., & Khan, I. (2019). Nanoparticles: Properties, applications and toxicities.

Arabian Journal of Chemistry, *12*(7), 908–931. https://doi.org/10.1016/j.arabjc.2017.05.011

L

Li, J., Liu, X., Zhang, Y., Tian, F., Zhao, G., Yu, Q., Jiang, F., & Liu, Y. (2012). Toxicity of nano zinc oxide to mitochondria. *Toxicology Research*, *1*(2), 137. https://doi.org/10.1039/c2tx20016c-Lozano, O., Silva-Platas, C., Chapoy-Villanueva, H., Pérez, B. E., Lees, J. G., Ramachandra,

C. J. A., Contreras-Torres, F. F., Lázaro-Alfaro, A., Luna-Figueroa, E., Bernal-Ramírez, J., Gordillo-Galeano, A., Benitez, A., Oropeza-Almazán, Y., Castillo, E. C., Koh, P. L., Hausenloy, D. J., Lim, S. Y., & García-Rivas, G. (2020). Amorphous SiO2 nanoparticles promote cardiac dysfunction via the opening of the mitochondrial permeability transition pore in rat heart and human cardiomyocytes. *Particle and Fibre Toxicology*, *17*(1), 15. https://doi.org/10.1186/s12989-020-00346-2

- Luaibi, N., & Zayed, N. (2018). Effect of ZnO NPs on Body and Organ Weights in Male Rats. *International Journal of Innovative Research in Computer and Communication Engineering*, *5*, 12–25.

- Luo, L., Ni, J., Zhang, J., Lin, J., Chen, S., Shen, F., & Huang, Z. (2024). Toosendanin induces hepatotoxicity by restraining autophagy and lysosomal function through inhibiting STAT3/CTSC axis. *Toxicology Letters*, *394*, 102–113. https://doi.org/10.1016/j.toxlet.2024.03.002

M

- Mailloux, R. J., Treberg, J., Grayson, C., Agellon, L. B., & Sies, H. (2023). Mitochondrial function and phenotype are defined by bioenergetics. *Nature Metabolism*, *5*(10), 1641–1641. https://doi.org/10.1038/s42255-023-00885-w

- Mallick, A., More, P., Syed, M. M. K., & Basu, S. (2016). Nanoparticle-Mediated Mitochondrial Damage Induces Apoptosis in Cancer. *ACS Applied Materials & Interfaces*, *8*(21), 13218–13231. https://doi.org/10.1021/acsami.6b00263

- MAT, M. (2023, April 9). *Nickel (Ni) Ore | Properties, Formation, Minerals, Deposits*. Geology Science. https://geologyscience.com/ore-minerals/nickel-ore/

- Muthuraman, A., & Kaur, J. (2017). Chapter 6 - Antimicrobial Nanostructures for Neurodegenerative Infections: Present and Future Perspectives. In A. Ficai & A. M. Grumezescu (Eds.), *Nanostructures for Antimicrobial Therapy* (pp. 139–167). Elsevier. https://doi.org/10.1016/B978-0-323-46152-8.00006-8

N

- Nickson, C. (2019, January 2). Mitochondrial dysfunction. *Life in the Fast Lane • LITFL*. https://litfl.com/mitochondrial-dysfunction/

- Nikolova, M. P., & Chavali, M. S. (2020). Metal Oxide Nanoparticles as Biomedical Materials. *Biomimetics (Basel, Switzerland)*, *5*(2), 27. https://doi.org/10.3390/biomimetics5020027

P

- Patrón-Romero, L., Luque-Morales, P. A., Loera-Castañeda, V., Lares-Asseff, I., Leal-Ávila, M. Á., Alvelais-Palacios, J. A., Plasencia-López, I., & Almanza-Reyes, H. (2022). Mitochondrial Dysfunction Induced by Zinc Oxide Nanoparticles. *Crystals*, *12*(8), 1089. https://doi.org/10.3390/cryst12081089

- Pereira, L. C., Pazin, M., Franco-Bernardes, M. F., Martins, A. D. C., Barcelos, G. R. M., Pereira, M. C., Mesquita, J. P., Rodrigues, J. L., Barbosa, F., & Dorta, D. J. (2018). A perspective of mitochondrial dysfunction in rats treated with silver and titanium nanoparticles (AgNPs and TiNPs). *Journal of Trace Elements in Medicine and Biology*, *47*, 63–69. https://doi.org/10.1016/j.jtemb.2018.01.007

R

- Rabinovich, A., Di, R., Lindert, S., & Heckman, J. (2024). Nickel and Soil Fertility: Review of Benefits to Environment and Food Security. *Environments*, *11*(8), Article 8. https://doi.org/10.3390/environments11080177

- Rouabhi R., Gasmi S., Boussekine S., Kebieche M .2015. Hepatic oxidative stress induced by zinc and opposite effect of selenium in oryctolagus cuniculus. Journal Environ Anal Toxicol 5: 289-298

S

- Sahu, D., Kannan, G. M., Vijayaraghavan, R., Anand, T., & Khanum, F. (2013). Nanosized Zinc Oxide Induces Toxicity in Human Lung Cells. *ISRN Toxicology*, *2013*, 1–8. https://doi.org/10.1155/2013/316075

- Salata, O. V. (2004). Applications of nanoparticles in biology and medicine. *Journal of Nanobiotechnology*, *2*(1), 3. https://doi.org/10.1186/1477-3155-2-3

- Salzillo, A., Ragone, A., Spina, A., Naviglio, S., & Sapio, L. (2023). Forskolin affects proliferation, migration and Paclitaxel-mediated cytotoxicity in non-small-cell lung cancer cell lines via adenylyl cyclase/cAMP axis. *European Journal of Cell Biology*, *102*(2), 151292. https://doi.org/10.1016/j.ejcb.2023.151292

- Siddiqui, M. A., Ahamed, M., Ahmad, J., Majeed Khan, M. A., Musarrat, J., Al-Khedhairy, A. A., & Alrokayan, S. A. (2012). Nickel oxide nanoparticles induce cytotoxicity, oxidative stress and apoptosis in cultured human cells that is abrogated by the dietary antioxidant curcumin. *Food and Chemical Toxicology*, *50*(3–4), 641–647. https://doi.org/10.1016/j.fct.2012.01.017

- Sies, H. (1999). Glutathione and its role in cellular functions. *Free Radical Biology and*

Medicine, *27*(9–10), 916–921. https://doi.org/10.1016/S0891-5849(99)00177-X

- Sies, H. (2020). Oxidative Stress: Concept and Some Practical Aspects. *Antioxidants*, *9*(9), Article 9. https://doi.org/10.3390/antiox9090852

- Smiley, S. T., Reers, M., Mottola-Hartshorn, C., Lin, M., Chen, A., Smith, T. W., Steele, G. D., & Chen, L. B. (1991). Intracellular heterogeneity in mitochondrial membrane potentials revealed by a J-aggregate-forming lipophilic cation JC-1. *Proceedings of the National Academy of Sciences*, *88*(9), 3671–3675. https://doi.org/10.1073/pnas.88.9.3671

- Song, M., Rosenthal, M., Song, A., Uyemura, K., Yang, H., Ament, M., Yamaguchi, D., & Cornford, E. (2009). Body weight reduction in rats by oral treatment with zinc plus cyclo- (His-Pro). *British Journal of Pharmacology*, *158*(2), 442–450. https://doi.org/10.1111/j.1476-5381.2009.00201.x

T

- *The Roles of Mitochondrial to Chronic Kidney Disease*. (n.d.). Retrieved March 23, 2025, from https://encyclopedia.pub/entry/15396

V

- Viala, A., & Botta, A. (2005). *Toxicologie* (2e éd.). Éd. Tec & doc Éd. médicales internationales.

W

- Waris, A., Sharif, S., Naz, S., Manzoor, F., Rashid, F., Tabassum, S., Jamil, F., Hussain, M., Choi, Y. J., & Park, Y.-K. (2023). Review on metallic nanoparticles induced toxicity on renal

function and overall health of kidneys. *Environmental Engineering Research*, *29*(4), 230549–0. https://doi.org/10.4491/eer.2023.549

- Weckbecker, G., & Cory, J. G. (1988). Ribonucleotide reductase activity and growth of glutathione-depleted mouse leukemia L1210 cells in vitro. *Cancer Letters*, *40*(3), 257–264. https://doi.org/10.1016/0304-3835(88)90084-5

Y

- Yang, K., Li, T., Geng, Y., Zou, X., Peng, F., & Gao, W. (2024). The role of mitophagy in the development of chronic kidney disease. *PeerJ*, *12*, e17260. https://doi.org/10.7717/peerj.17260

- Yin, H., Li, X., Wang, C., Li, X., & Liu, J. (2024). Nickel induces mitochondrial damage in renal cells in vitro and in vivo through its effects on mitochondrial biogenesis, fusion, and fission. *Chemico-Biological Interactions*, *394*, 110975. https://doi.org/10.1016/j.cbi.2024.110975

- Yu, S., Liu, F., Wang, C., Zhang, J., Zhu, A., Zou, L., Han, A., Li, J., Chang, X., & Sun, Y. (2018). Role of oxidative stress in liver toxicity induced by nickel oxide nanoparticles in rats. *Molecular Medicine Reports*, *17*(2), 3133–3139. https://doi.org/10.3892/mmr.2017.8226

-

Z

- Zhang, N., Xiong, G., & Liu, Z. (2022). Toxicity of metal-based nanoparticles: Challenges in the nano era. *Frontiers in Bioengineering and Biotechnology*, *10*. https://doi.org/10.3389/fbioe.2022.1001572

- Zhang, W., Gao, J., Lu, L., Bold, T., Li, X., Wang, S., Chang, Z., Chen, J., Kong, X., Zheng, Y., Zhang, M., & Tang, J. (2021). Intracellular GSH/GST antioxidants system change as an earlier biomarker for toxicity evaluation of iron oxide nanoparticles. *NanoImpact*, *23*, 100338. https://doi.org/10.1016/j.impact.2021.100338

- Zhang, Z., Miao, G., Lu, L., Yin, H., Wang, Y., Wang, B., Pan, R., Zheng, C., & Jin, X. (2024). Crucial physicochemical factors mediating mitochondrial toxicity of nanoparticles at noncytotoxic concentration. *The Science of the Total Environment*, *908*, 168211. https://doi.org/10.1016/j.scitotenv.2023.168211

- Zhuo, L.-B., Liu, Y.-M., Jiang, Y., & Yan, Z. (2024). Zinc oxide nanoparticles induce acute lung injury via oxidative stress-mediated mitochondrial damage and NLRP3 inflammasome activation: In vitro and in vivo studies. *Environmental Pollution*, *341*, 122950. https://doi.org/10.1016/j.envpol.2023.122950

-